# The large eddies of turbulent motion

By H. L. GRANT*
*Cavendish Laboratory, University of Cambridge*

(*Received* 16 *December* 1957)

CONTENTS



SUMMARY

This paper describes an experimental investigation of the form of the large scale motions in turbulent flow. These motions have been found to be more ordered than has usually been supposed and their origin and dynamics are discussed in terms of physical models of typical eddies.

Nine components of the double velocity correlation tensor have been measured at a number of positions in the wake of a circular cylinder and in a 'flat plate' boundary layer. These

* Present address : Pacific Naval Laboratory, Esquimalt, B.C., Canada.

have been supplemented by measurements of correlations with separations in directions other than the axial ones. In the wake, the correlations at large values of the separation are explained in terms of two types of large scale motion. One of these is a pair of vortices, side by side and rotating in opposite directions with axes aligned approximately normal to the plane of the wake. The other typical motion is a series of jets in which turbulent fluid is projected outward from the core of the wake. It is suggested that these are the result of an instability of the turbulent shear stress. A qualitative explanation of the apparent structural equilibrium of the wake is given in terms of this instability. The vortex pair eddies were not found in the boundary layer but there is evidence of jets much like those in the wake.

Correlations measured in grid turbulence have been found to be highly anisotropic and consistent with the presence of vortex pair eddies. When a plane strain was applied to grid turbulence, the effect on the correlations suggested the presence of a stress instability similar to that postulated for the wake.

## 1. Introduction

Townsend's (1956) measurements of the 'transverse double velocity correlation' in the turbulent wake of a circular cylinder have made it clear that a certain amount of order exists in the largest eddies in this flow. Using the downstream component of turbulent velocity, he found that the transverse correlation was positive for all values of the separation in the direction normal to the plane of the wake but was negative for large values of the separation in the direction parallel to the plane of the wake. These observations were interpreted in terms of a set of large eddies, rotating about axes in the direction of the mean flow and with planes of circulation inclined so that the mean shear acted to decrease the area of circulation and increase the energy of the eddy. It was postulated that the average eddy was in energy equilibrium, gaining energy from the mean flow at the same rate as it was lost through the working of the Reynolds stresses of the more disorganized turbulence.

This interpretation described the available data from the wake plausibly enough but the almost complete lack of comparable experimental observations in other turbulent shear flows suggested the need for a more detailed examination of the correlation. This paper describes measurements of nine components of the double velocity correlation in a turbulent wake and a turbulent boundary layer. The results are used to form a new physical model of the largest eddies in the flow.

## 2. Experimental procedure

### 2.1. *Coordinate system*

Cartesian coordinates are appropriate to all of the flows that are being considered. In the wake, the $x$-axis is parallel to the axis of the cylinder,

which lies in a direction normal to the free stream. The $x$-axis is in the plane of symmetry in the direction of the free stream and $x$ is increasing in the direction of the mean flow. The $y$-direction is normal to the plane of symmetry.

In the boundary layer, the $y$-axis is normal to the wall and the $x$-axis lies in the wall in such a way that the direction of the mean velocity is parallel to the $(x, y)$-plane. The $z$-direction is also in the wall and normal to the $x$-axis. In the case of the square mesh grid, the $x$-axis is in the direction of the mean velocity, the $z$-axis parallel to the trailing set of bars and the $y$-axis parallel to the leading set of bars.

The components of mean velocity in the $x$-, $y$-, $z$-directions respectively will be $U$, $V$, $W$, and the components of velocity fluctuation will be $u$, $v$, $w$. It is often convenient to use subscripts to distinguish between the directions, and the subscripts 1, 2, 3, will refer to the $x$-, $y$-, $z$-directions respectively.

2.2. *The double velocity correlation*

The quantity that has come to be known as the double velocity correlation in turbulence theory, is the covariance in statisticians' terminology. It will be written

$$R'_{ij}(\mathbf{x}, \mathbf{x}+\mathbf{r}) = \overline{u_i u'_j}$$

where $u_i$ is the $i$-component of turbulent velocity at a point $P$ with position vector $\mathbf{x}$, and $u'_j$ is the $j$-component of turbulent velocity at a point $P'$ with position vector $\mathbf{x}+\mathbf{r}$. The present discussion will be confined to cases where $i = j$.

It is easier to measure the correlation coefficient

$$\overline{u_i u'_j}/(\overline{u_i^2 u_j'^2})^{1/2}$$

which does not require absolute determination of the sensitivity of the hot wires, but the denominator of this quantity is, in general, a function of $r$. It is therefore preferable to replace the denominator by the intensity at the fixed probe. For brevity in what follows, the quantities like $R'_{ii}(x, y; r_1, r_2, r_3)/\overline{u_i^2}$, where $\overline{u_i^2}$ and $(x, y)$ are understood to refer to the fixed probe, will simply be written in the form

$$R_{ii}(r_1, r_2, r_3),$$

and will be referred to as 'correlations'.

It is sometimes difficult to think of an eddy as a clearly defined structure. In general we are forced to rely on the intuitive idea that the turbulence consists of superimposed motions of various length scales and to define an eddy as a region over which the turbulent velocity is correlated. It may then be assumed that the covariance between the velocities at two points is unaffected by motions which have length scales much smaller than the distance between the points $r$.

We may expect that the maximum length scale associated with the turbulence will be of the order of the largest length scale of the mean velocity

variation so it will be assumed that the covariance $\to 0$ as $r \to \infty$. This includes the assumption that any periodic motions which may be introduced into the turbulence do not extend very far in space without damping or change of phase. At the largest values of $r$ for which the covariance is non-zero, the covariance will be dominated by the effects of the largest eddies present and at any smaller value of $r$, the covariance will receive contributions from all motions with length scales greater than $r$. In the particular case where there is a set of eddies, an order of magnitude larger than any of the other turbulent motions which contain appreciable energy, these eddies alone will determine the covariance over a considerable range of $r$ at the end of the curve.

The most obvious conclusions that can be drawn from a knowledge of the correlations concerns the backflow required by continuity. It may be shown (Townsend 1956, p. 14) that for two points in a plane, the correlation between the turbulent velocity components normal to the plane must be negative for some values of the separation vector $\mathbf{r}$. For such values of $\mathbf{r}$, the instantaneous velocity at the two points is, on the average, in opposite directions and if $|\mathbf{r}|$ is large, the correlation is dependent only on the largest eddies. We can thus gain some qualitative information about the large eddies quite easily, but even the whole correlation tensor is not by any means a complete specification of the motion.

The one-dimensional spectra measured in the cylinder wake by Townsend (1950) show an appreciable peak at small wave-numbers fairly well separated on the wave-number axis from the broad peak which contains most of the energy in the spectrum. It will be shown later that the observed correlations show considerable variations of character at large $r$. These observations suggest the possibility of a fairly well-ordered set of large eddies with characteristic length scale large compared with the largest of the 'energy containing' eddies.

Since we cannot predict a unique set of large eddies from the correlations, we may only hope to make a convincing argument for a rather simple set of eddies which will yield quantitative agreement with a number of observed correlations with an equal or smaller number of adjustable constants. Even if we can find such a fit, with a small number of constants, it is desirable to have further evidence for the chosen form. This might be a physical argument showing how the form could arise and should include at least qualitative agreement with all measured correlations.

If the typical eddy can be expressed analytically, it is usually quite easy to calculate its contribution to the correlation. The essential assumptions are as follows.

1. The eddies are of a size much larger than any other component of the turbulence.
2. The eddies are placed at random in the $(x, y)$-plane. (In most shear flows, there will have to be restrictions on the location of the eddies in the $y$-direction. In a two-dimensional flow, the largest eddies may be comparable in size with the thickness of the turbulent

region so we must assume that all of the large eddies are located within a limited region on the $y$-axis.)

3. The motions of adjacent or overlapping eddies are independent. (This ensures that any contribution to the correlation comes from a single eddy.)

Experience has shown that when a large set of measured correlations is available, only a very few kinds of simple eddy can yield correlations with the right sign at large $r$. The sign of the expected correlation is easily determined without any calculation at all, simply by looking at a model of the assumed big eddies. One simply chooses two points on opposite sides of the model, separated in the direction corresponding to the correlation under consideration and notes whether or not the velocity component has the same direction at the two points.

### 2.3. *Experimental equipment*

The wind-tunnel used for measurement of wake and grid turbulence is a small closed return tunnel with a contraction ratio of 9:1 built and described by McPhail (1944). It has a working section 38 cm square and 160 cm long. The tunnel used for most of the boundary layer work had its origin in the duct used by Townsend (1954) to distort grid turbulence by the application of a plane shear. It has undergone many changes since then but still retains the one-dimensional contraction and the motor section described by Townsend. Between these, there now exists a duct 106 in. long and approximately 24 in. × 6 in. in cross-section. The cross-sectional area of the duct is constant for the first 50 in. and then increases gradually to compensate for the growth of the boundary layers. The roof has been made adjustable in this latter region and has been arranged so that there is no longitudinal pressure gradient in the boundary layer on the floor. There is a small trip fence on the floor at the exit of the contraction to ensure uniform transition and to thicken the boundary layer.

The hot wires were made of platinum-cored Wollaston wire, etched after being soldered in place. The diameter was 0·00025 cm (after etching); the length of the wire was typically 0·05 cm and never exceeded 0·1cm. Two forms of sensitive element were used: a single straight wire placed normal to the stream (U-wire) for measuring the downstream component of turbulent velocity, and a pair of wires in the form of an X (X-wire) for the cross-stream components. Because of the need to bring X-wires into close proximity with each other and with a wall, it was necessary to construct several novel forms of wire holder. The only special technique required, however, is patience.

### 2.4. *Accuracy of the correlation measurements*

The discussion that follows is confined to the part of the correlation curves for which $r$ is greater than 1·5 cm. As this is about 30 times the wire length, no wire length corrections have been necessary. There is

also no need for precise compensation of each of the four hot wires. The response of the wires is significantly non-linear in the boundary layer very near the wall but the effect on the correlation does not amount to more than about 5%, which is not important in the small correlations found in this situation at large values of $r$.

The largest errors arise in the taking of averages. By averaging over a sufficient time, it is possible to determine the correlation at a given pair of points to a fraction of 1% but in order to save time in a long series of measurements, it is necessary to use averages which are sufficiently accurate for the purpose in hand but not necessarily the best that can be obtained. Generally the averaging time was adjusted to yield a probable error of about $\pm 0{\cdot}01$ for correlations larger than 20% and decreasing for smaller correlations so that values of less than 0·01 have a probable error of about 0·002.

Exceptions to the above estimates must be made for correlations with separations in the $x$-direction. In these cases, it is almost impossible to avoid some interference at the downstream wire from the wake of the upstream one. The procedure which has been adopted to minimize this effect has been to mount the sensitive part of the upstream wire on long lengths of Wollaston wire so that it stands out about 0·5 cm from the heavy supports. The track followed by the moving (downstream) wire passes within a few tenths of a millimetre on the side away from the supports. For values of $r$ less than about 2 cm, the signal from the downstream wire shows some very high frequency components when viewed with an oscilloscope and peculiar effects are found in some of the measured correlations. The correlations in this region are very sensitive to slight transverse movements of the downstream wire and are not very reliable. At about $r = 2$ cm, the wake of the Wollaston wire appears to decay to the extent that its effects are negligible and the measured correlations become quite reproducible. This condition lasts until about 6 cm downstream where the wake of the wire supports in the leading probe begins to interfere. The errors in the observations are less serious in this region because this wake can be avoided by moving the trailing probe a short distance in a transverse direction. The line joining the two probes changes direction by only two or three degrees.

## 3. The wake of a circular cylinder

### 3.1. *Correlations in the cylinder wake*

The measurements to be considered have been made with the fixed probe at a distance of 533 diameters behind a circular cylinder at a Reynolds number of 1300 ($U = 625$ cm/sec, $d = 0{\cdot}317$ cm). The mean velocity distribution was measured with a total head tube of 1 mm outside diameter and is given in figure 1. The diameter of the cylinder ($d$) will be used as a unit of length and figure 1 serves to show the width of the wake in these units. The width of the intensity distributions can be compared with that

of the mean velocity distribution by reference to a comprehensive set of intensity measurements given by Townsend (1956).

The nine quantities $R_{ii}(y; r_1, r_2, r_3)$ are shown in figure 2 for cases where the separation $r$ is in one of the coordinate directions. Each component has been determined with the fixed probe at three distances from the centre of the wake. One position is at the centre, one at 4 cylinder diameters from the centre which, at this value of $x$, is near the point of maximum shear, and one at 7·6 diameters which is near the outside edge of the wake but at a point where an appreciable signal can still be obtained.

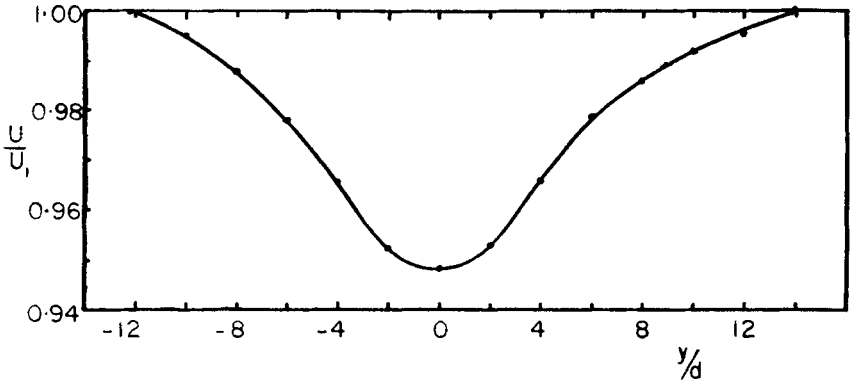


Figure 1. The mean velocity profile in the cylinder wake at $x/d = 533$.

These curves exhibit a wide variety of forms at large values of $r$. This suggests the presence of rather simple eddy structures because in a very confused turbulence the characteristics of any particular motion which does not appear frequently with a fixed orientation would be expected to disappear in the averaging, leading to smooth correlation curves with considerable symmetry. In isotropic turbulence, for example, continuity and symmetry require the '$g(r)$-type' correlations (separation vector normal to the velocity component) to be identical and to be negative at some values of $r$. It is almost certain that these negative values would occur at the largest values of $r$ for which the covariance is non-zero. The remaining correlations, which have the separation vector parallel to the velocity component, will be equal to each other. No proof has been given that they remain positive but this would seem to be the simplest physical situation and therefore perhaps the most likely.

Examination of figure 2 will show that the observed correlations in the cylinder wake are very different from what is expected in isotropic turbulence. $R_{33}(0, 0, r)$ is negative for all values of $y$. When the fixed point is near the outside of the wake, $R_{11}(0, r, 0)$ has a minimum and $R_{33}(0, r, 0)$ goes strongly negative and then takes positive values as $r$ increases. $R_{11}(0, 0, r)$, $R_{22}(r, 0, 0)$, and $R_{33}(r, 0, 0)$ also have negative values followed by positive ones, at least for the larger values of $y$, but $R_{22}(0, 0, r)$ is independent of $y$ and never negative.

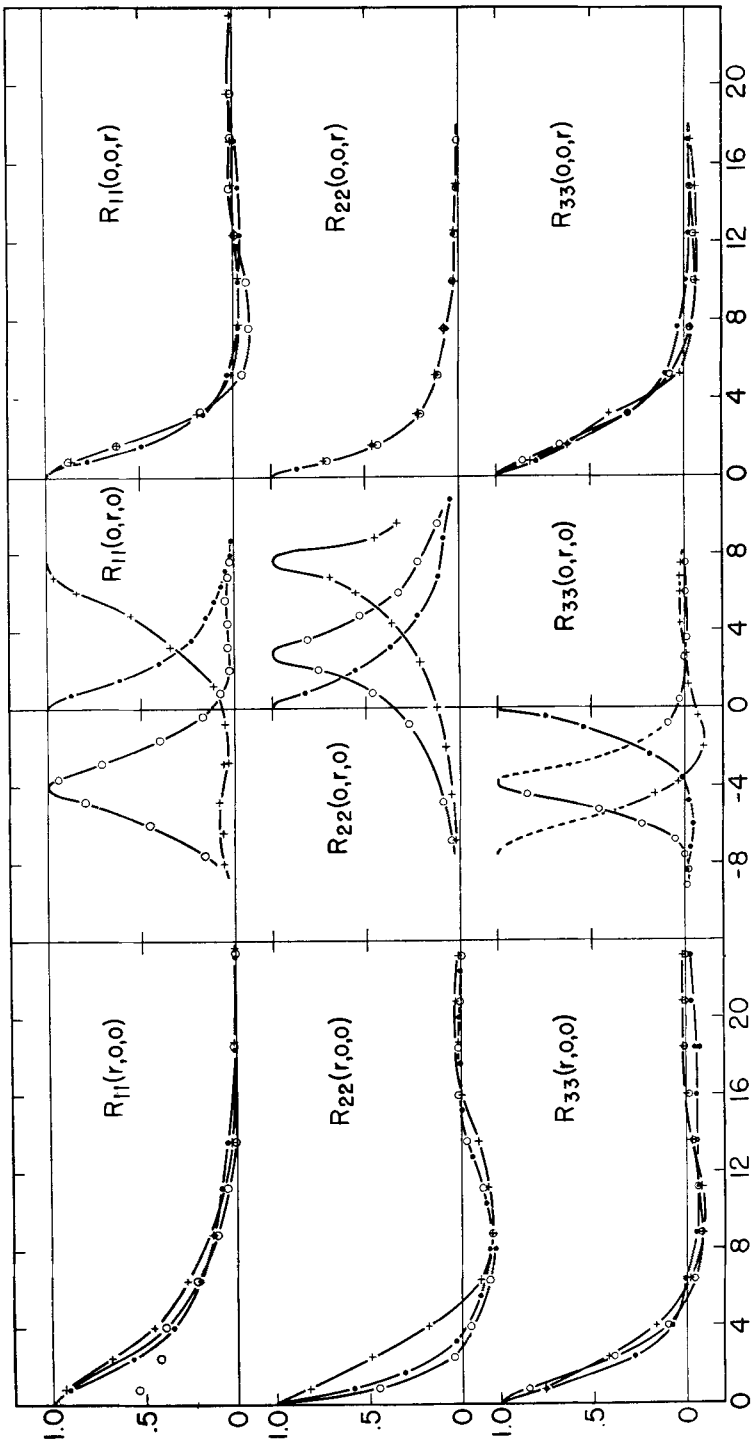


Figure 2. The nine correlations in the cylinder wake. The measurements were made with the fixed probe at three values of $y$: ● $y/d = 0$, ○ $y/d = 4$, + $y/d = 7{\cdot}6$. (Except $R_{22}(0, r, 0)$ where the positions are 0, 2·8, 7·6 respectively.)

3.2. *The vortex pair eddies*

As a first attempt to interpret these curves, I searched for a set of a single kind of large eddy which would account for all of the observed correlations at large values of $r$. It is clear that the type of eddy chosen by Townsend is not satisfactory because it is very long in the $x$-direction and its velocities are independent of $x$. This would lead to positive values of $R_{22}(r,0,0)$ and $R_{33}(r,0,0)$. There is a component of vorticity in the $x$-axis which would lead to negative values of $R_{22}(0,0,r)$ which are not observed. It may also be noted that the correlations with separation in the $y$-direction all show significant non-zero values when the probes are in opposite sides of the wake.

About the simplest kind of big eddy that we might hope to discover would be a body of fluid rotating about an axis, but not as a rigid body and with its circulation not necessarily in planes normal to the axis. Townsend's eddies are of this sort. The obvious difficulty in trying to produce the desired correlations from a distribution of these eddies is the observed values of $R_{33}(0,0,r)$. There are certain configurations within the above definition of a simple eddy which can give negative values of $R_{33}(0,0,r)$ but they require quite narrow restrictions on the orientation of the axis of the eddy and the planes of circulation with respect to the coordinate axes. It is doubtful if they could produce negative values over a large enough range of $r$, and in any case these eddies seem inevitably to produce negative values of $R_{22}(0,0,r)$.

A more likely way to get negative values of $R_{33}(0,0,r)$ at large $r$, is to have pairs of simple eddies side by side and rotating in opposite directions. Again it is not possible to make a simple distribution of these eddies which will yield all the observed correlations at large $r$. Some progress can be made, however, if we assume that there exists a set of adjacent pairs of eddies in which the circulation is always in the $(x,z)$-plane. These contain no $v$ component of velocity and so only the affect $R_{11}$ and $R_{33}$ correlations. This type of eddy is illustrated schematically in figure 3. The arrows indicate the direction of the local velocity in the eddy and it can be seen that $R_{11}(0,0,r)$ will be negative and then positive as $r$ increases; $R_{11}(r,0,0)$ will always be positive. The bend in the axes of the eddy is needed for a qualitative explanation of the correlations with separations in the $y$-direction. It would be expected to produce a minimum in $R_{11}(0,r,0)$ when the fixed point is in the outer part of the wake, and a negative region in $R_{33}(0,r,0)$.

This eddy contains no $v$ component and the correlations with separation in the $(x,z)$-plane will be independent of assumptions about the shape of the bend caused by the mean velocity if this is produced by a simple translation. Thus we may calculate the correlations with separations in this plane from a model in which the axes of rotation are straight and in the $y$-direction. Such an eddy may be described by

$$u = A(1-\alpha^2 z^2)\exp\{-\tfrac{1}{2}\alpha^2(x^2+z^2)\}$$

and

$$w = A\alpha^2 xz\exp\{-\tfrac{1}{2}\alpha^2(x^2+z^2)\}.$$

Assuming a uniform distribution of these eddies over the wake, we may calculate their contribution to the correlations. The results are as follows:

$$R_{11}(r,0,0) = a_1 \exp(-\tfrac{1}{4}\alpha^2 r^2),$$
$$R_{11}(0,0,r) = a_1\{1-\alpha^2 r^2+\tfrac{1}{12}\alpha^4 r^4\}\exp(-\tfrac{1}{4}\alpha^2 r^2),$$
$$R_{33}(r,0,0) = R_{33}(0,0,r) = a_3\{1-\tfrac{1}{2}\alpha^2 r^2\}\exp(-\tfrac{1}{4}\alpha^2 r^2).$$

In these expressions, $a_1$ and $a_3$ are the proportion of $\overline{u^2}$ and $\overline{w^2}$ respectively which are contributed by the big eddies. If we set $a_1 = a_3 = 0{\cdot}13$, and $\alpha d = 0{\cdot}25$, these expressions fit the observations remarkably well as shown in figure 4. The order of magnitude of the constants is quite believable but it is a little hard to justify putting $a_1 = a_3$. The intensities due to the big eddies are

$$\overline{u_b^2} = \overline{A^2}\frac{3\pi}{4\alpha^2} \quad \text{and} \quad \overline{w_b^2} = \overline{A^2}\frac{\pi}{4\alpha^2}.$$

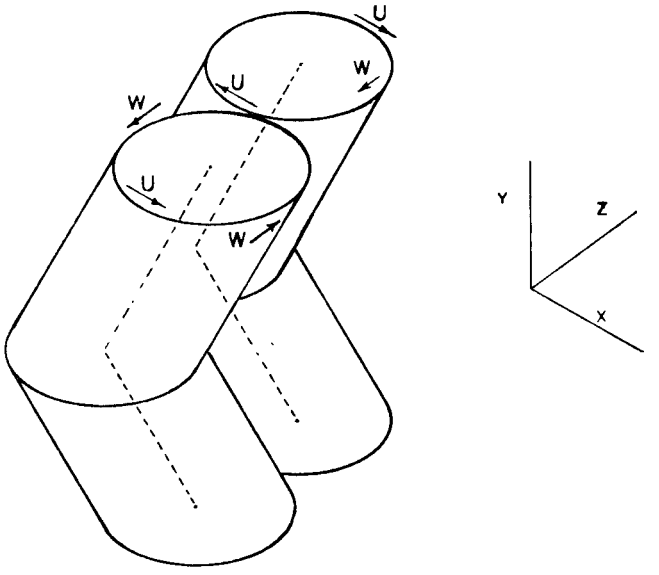


Figure 3. Schematic model of the vortex pair eddy.

We have then

$$\overline{w_b^2} = \tfrac{1}{3}\overline{u_b^2}.$$

Now from values of $\overline{u^2}/U^2$ and $\overline{w^2}/U^2$ published by Townsend (1956, pp. 142–3), $\overline{w^2}/\overline{u^2}$ is found to be 0·88 at $y/d = 4$, but his X-wire was calibrated on the assumption that grid turbulence is isotropic and the most probable value is about 75% of this (Grant & Nisbet 1957) which gives $\overline{w^2}/\overline{u^2} = 0{\cdot}66$. We now have $3 \times 0{\cdot}66(\overline{w_b^2}/\overline{w^2}) = \overline{u_b^2}/\overline{u^2}$, or $a_3 = \frac{1}{2}a_1$. This is a rather uncertain calculation but it indicates that the assumed eddy does not fit quite as well as is implied by figure 4. However, even if the

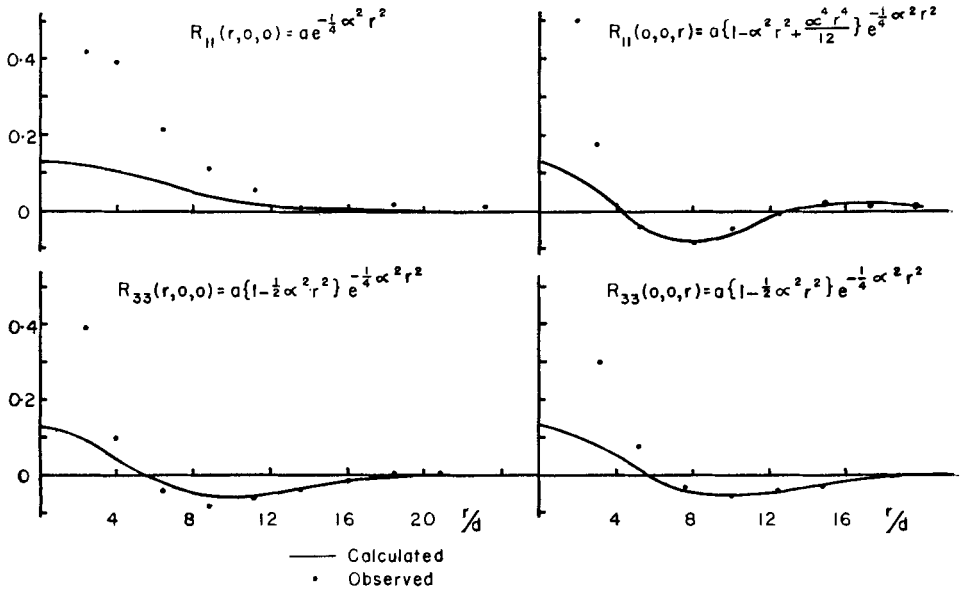


Figure 4. Correlations from the vortex pair eddies; — calculated, ● observed.

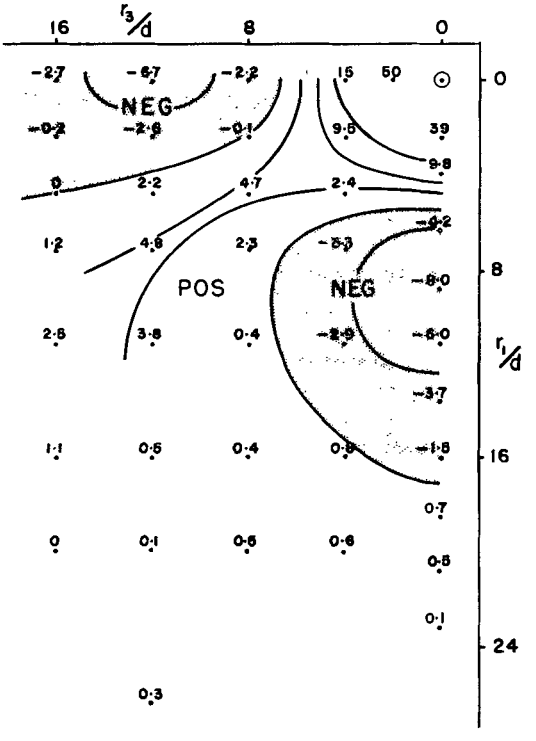


Figure 5. Contour plot of $R_{33}(r_1, 0, r_3)$ expressed as percentage. $y/d = 4$.

condition $a_3 = \frac{1}{2}a_1$ is imposed upon the calculated correlation, there will still be quite a reasonable fit.

It can be seen from figure 3 that although $R_{33}(r,0,0)$ and $R_{33}(0,0,r)$ are negative for some values of $r$, $R_{33}$ should be positive for all values of separation in directions approximately at 45° to the $x$- and $z$-axes in the $(x,z)$-plane. This has been tested by fixing one probe in the plane $y/d = 4$ and moving the other over that plane. The result is shown in figure 5 which is strong evidence that the eddy that has been assumed to be responsible for the correlations in the $(x,z)$-plane is qualitatively correct.

The correlations with separation in the $y$-direction are more difficult to explain quantitatively by this model. The search for an analytical description of the model is hampered by the need to make assumptions about the way in which the energy falls off with $y$, and about the shape of the axis of the eddy in the $(x,y)$-plane. Since the wake is not even approximately homogeneous in the $y$-direction, we may also have to assume a frequency distribution describing the probability of the centre of the eddy being located at a given value of $y$. It cannot be assumed that all eddies are symmetrical about the central plane of the wake because that would require the correlation caused by the big eddies to be symmetrical about $y = 0$ also. For the fixed wire at $y/d = 4$, we would expect that $R_{11}(0,r,0)$ and $R_{33}(0,r,0)$ would be approximately 0·13 at $r/d = -8$. This is clearly not so (figure 2). An attempt was made to fit the observations by assuming the eddies to be of the form

$$u = A(1-\alpha_1^2 z^2)\exp\{-\tfrac{1}{2}\alpha_1^2[(x-by^2)^2+z^2]-\tfrac{1}{2}\alpha_2^2(y-y_0)^2\},$$
$$w = A\alpha_1^2(x-by^2)z\exp\{-\tfrac{1}{2}\alpha_1^2[(x-by^2)^2+z^2]-\tfrac{1}{2}\alpha_2^2(y-y_0)^2\}.$$

Here we have assumed a parabolic form for the bend in the eddy and an exponential decay of energy in the $y$-direction. In taking averages, $y_0$ was assumed to be uniformly distributed which is unrealistic in the outer part of the wake because, at $y/d = 8$, the total intensity is less than 13% of the intensity at the centre while this assumption makes the intensity of the big eddies constant. The result could not be made to give satisfactory agreement with the observations even for $y/d = 4$. Since we already have two constants, $\alpha_2$ and $b$, which are adjustable over a considerable range, there is not likely to be much profit in trying to refine the specification, as this would almost certainly introduce more unknown constants and eventually lead to agreement with the observations regardless of the real physical situation.

$R_{33}$ was measured with one probe fixed at the outside edge of the wake ($y/d = 7{\cdot}6$) and the other moving over the $(x,y)$-plane. The contours of zero correlation are shown in figure 6. The shape of the region of positive correlation is about what is expected from the postulated model and indicates that the axes of the eddy are at about 45° to the coordinate axes. The turning points in the zero correlation contours are not at the centre of the wake but the reason for this can be seen if the data are plotted differently.

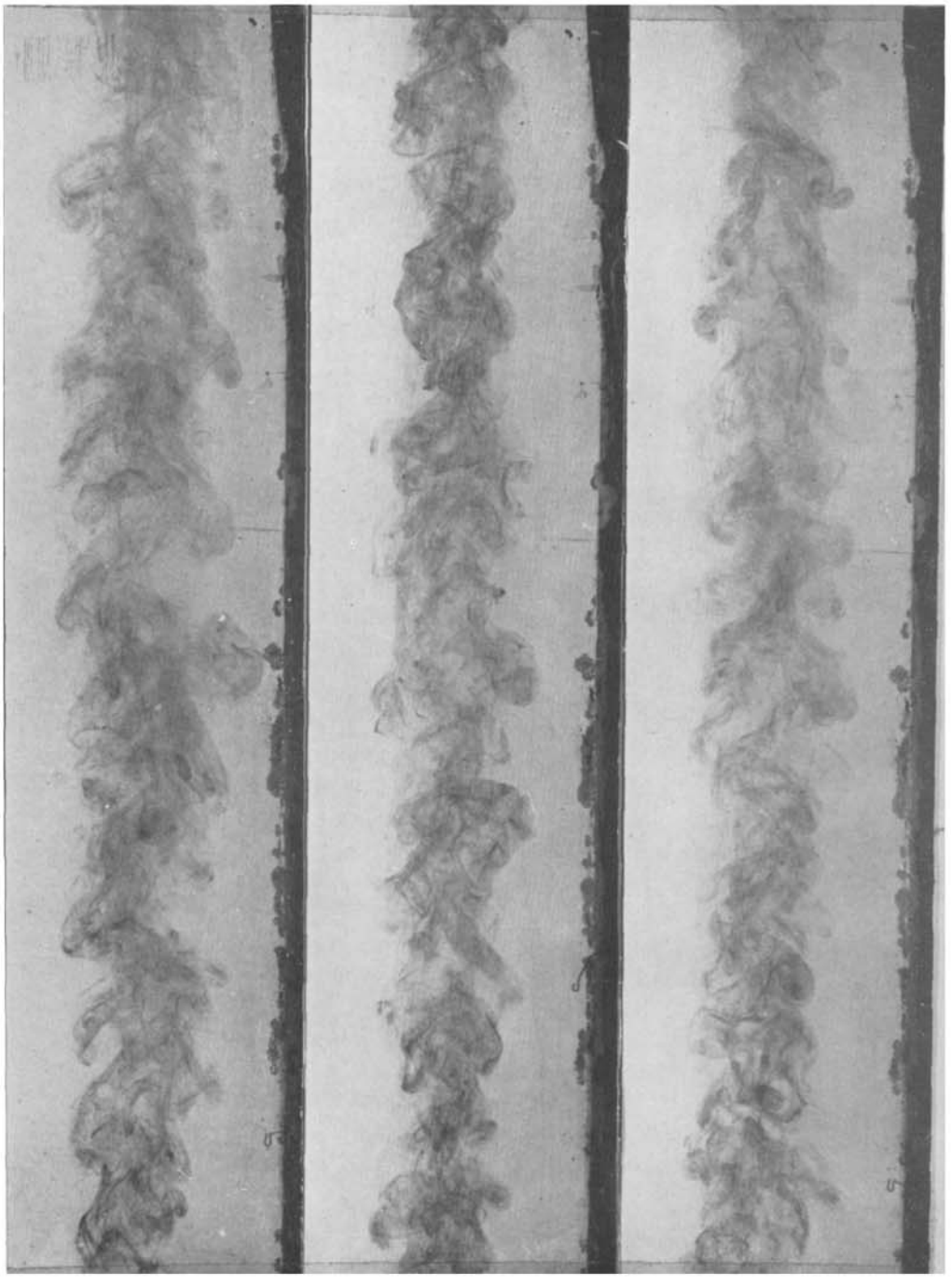

Figure 11. Wakes produced by cylinder moving from left to right through still water. Coloured fluid was emitted from a short section near the centre of the cylinder.

In figure 7 and several subsequent figures, the data are presented in a manner which is more useful for some purposes than the contour plot. The measurements were made by fixing one probe at a point in the

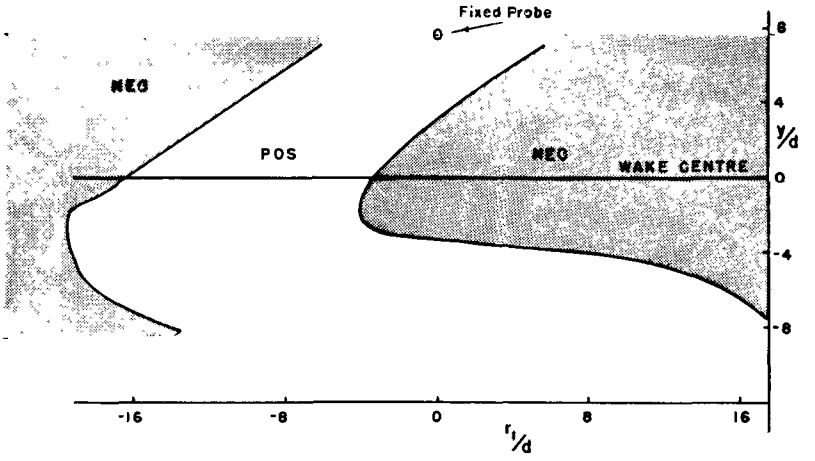


Figure 6. Zero correlation contours for $R_{33}(r_1, r_2, 0)$ with the fixed probe at $y/d = 7{\cdot}6$ The scale of $y/d$ refers to the moving probe.

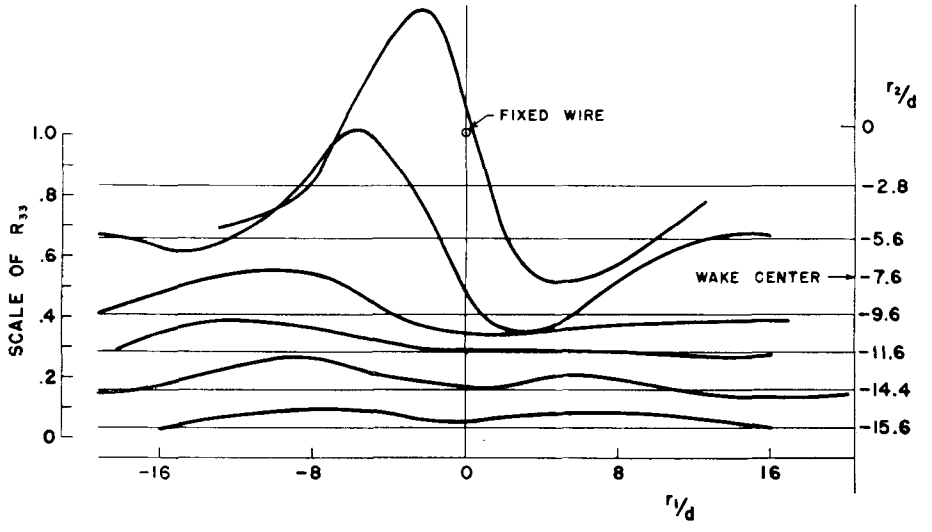


Figure 7. Sections of the surface representing $R_{33}(r_1, r_2, 0)$ with the fixed probe at $y/d = 7{\cdot}6$. The fixed probe and the straight lines followed by the moving probe are shown in their correct positions in the $(r_1, r_2)$-plane. The correlation is plotted with these lines as axes.

$(x, y)$-plane and moving the other along lines $y =$ constant. In the figure, the position of the fixed probe, and the lines followed by the moving probe are shown in the $(r_1, r_2)$-plane. Each traverse of the moving probe along

a line $y$ = constant, determines a section of the correlation surface and these sections are plotted, using the corresponding lines as axes. The scale for the correlation curves is shown at the left side of the figure.

In figure 7, it can be seen that, at large values of $r_2$, the curves have the shape which would be expected from a superposition of the correlation due to the vortex pair eddies and a negative correlation in the region around $r_1 = 0$. This is clearly the reason why $R_{33}(0, r, 0)$ does not rise to something like 0·13 when the probes are at $y/d = 8$ and $y/d = -8$. The physical interpretation of this additional correlation is open to question, but it is most likely indicative of a tilt in the stress releasing motions which will be discussed in § 3.5. The effect appears to be too localized to be caused by disorganized turbulence of this scale but the possibility of large eddies rotating about axes in the $x$-direction at the centre of the wake could only be ruled out by a detailed study of $R_{22}(0, r_2, r_3)$ which has not been made. There is, however, no further positive evidence to suggest such a motion.

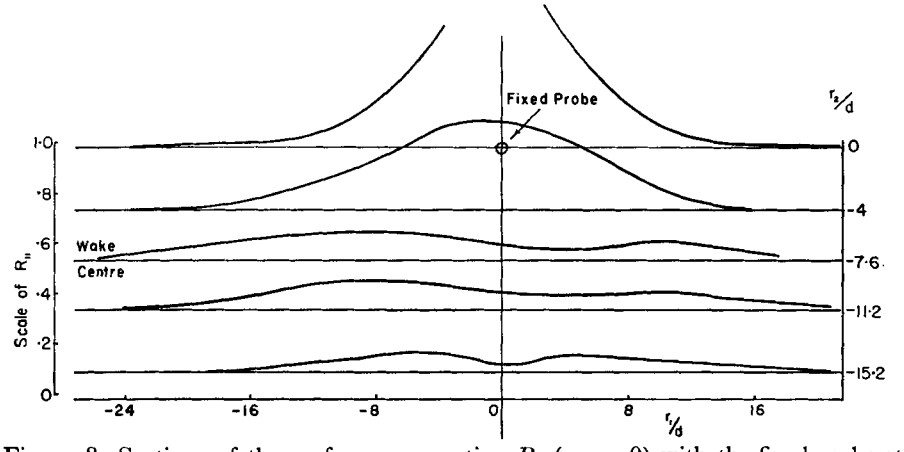


Figure 8. Sections of the surface representing $R_{11}(r_1, r_2, 0)$ with the fixed probe at $y/d = 7{\cdot}6$.

The distribution of $R_{11}$ in the $(x, y)$-plane with the fixed probe again at $y/d = 7{\cdot}6$ is shown in figure 8. The pattern is more complex than would be expected from the big eddies under discussion. It does, however, show a maximum correlation which is displaced in the upstream direction at the centre of the wake by about the same distance as the maximum correlation in the $R_{33}$ plot. When the moving probe is in the other side of the wake, there is again a negative correlation, centred on the line $x = 0$, superimposed on the correlation due to the vortex pair eddies. Before we can attempt to interpret this, we must consider the correlations involving the $v$ component of velocity.

### 3.3. *The mixing jets*

The $R_{22}$ correlations for separations in the axial directions are shown in figure 2. The interesting points include the large negative values of

$R_{22}(r, 0, 0)$ followed by positive values, the lack of negative values of $R_{22}(0, 0, r)$ and the fact that $R_{22}(0, 0, r)$ extends for a comparatively short distance on the $r$-axis and is independent of $y$. Figures 9 and 10 illustrate

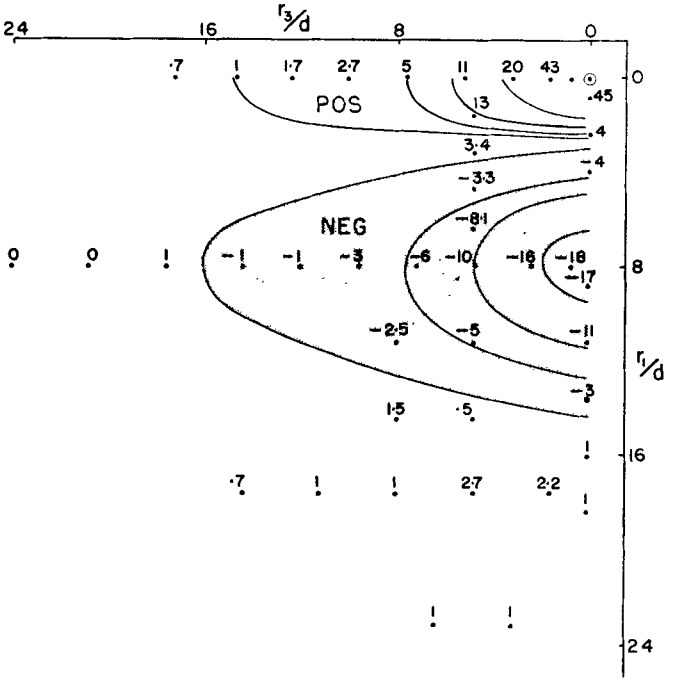


Figure 9. Contour plot of $R_{22}(r_1, 0, r_3)$ at $y/d = 4$.

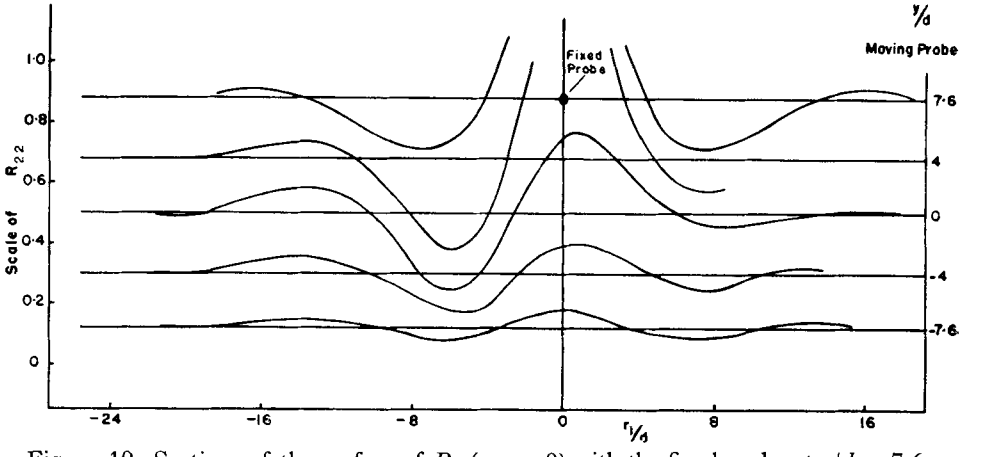


Figure 10. Sections of the surface of $R_{22}(r_1, r_2, 0)$ with the fixed probe at $y/d = 7{\cdot}6$.

the distribution of $R_{22}$ in the $(x, y)$-plane at $y/d = 4$ and in the $(x, z)$-plane with the fixed probe at $y/d = 7{\cdot}6$. The first of these figures clearly indicates rotation about axes in the $z$-direction. The second suggests a structure

which is nearly periodic in the $x$-direction. In this case, the correlation is very asymmetrical when the moving probe is at the centre of the wake but there is not any shift in phase such as would be expected if a simple structure were being distorted by the mean velocity distribution. The periodic part, then, must arise locally or move along with the speed of the free stream. The largest negative values of the correlation are centred roughly on the line along which $R_{11}$ and $R_{33}$ are most positive. This is probably only a coincidence as the positive peaks are also higher on the upstream side of the fixed probe and there is no obvious way to alter the model of the vortex pair eddies to include negative values of $R_{22}$ along this line. On the whole, the $R_{22}$ correlations appear to be the result of a different type of large scale motion with velocities mainly in the $y$-direction and with an approximate periodicity for short distances in the $x$-direction.

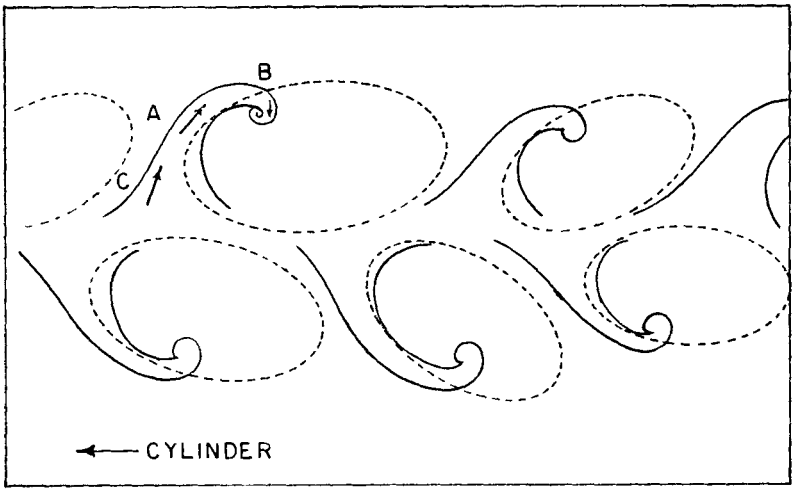


Figure 12. Sketch of a jet system in a late stage of development.

At this point it is convenient to refer to experiments in which a circular cylinder emitting a small quantity of coloured fluid was moved through still water. The cylinder was $\frac{1}{8}$ in. in diameter and 6 in. long and was moved through a long glass-sided tank with cross-sectional dimensions 6 in. $\times$ 6 in. The Reynolds number was about 800. The observer of this wake is in a position equivalent to that of moving with the stream in the wind-tunnel situation and he is able to see quite well the development of the outer part of the wake with time. Looking in the $z$-direction, the most obvious large scale motion in the outer part of the wake is a series of more or less regularly spaced 'jets' of turbulent fluid proceeding outward from the central plane of the wake. Typical photographs are shown in figure 11 (plate 1). From direct observation of the developing wake and from motion pictures, it appears that a series of jets in a late stage of development is part of a system similar to the one sketched in figure 12. The dashed lines

represent irrotational motions which rarely make a complete revolution. The structure is only approximately periodic, and as time goes on and successive 'jets' arise and decay, the typical 'wavelength' increases.

This is obviously the sort of structure needed to produce the heavily damped periodicity in $R_{22}$ but we must also consider the meaning of the asymmetry. It is observed in the tank that, when a jet is fully developed, the region of the turbulent core from which it arose has been displaced appreciably in the direction toward the cylinder. It may therefore be expected that the motion in the outer part of a jet is more closely connected to motions in the centre of the wake which are slightly upstream. The periodicity clearly indicates that the correlations extend over more than one jet, but if the structure of the jets is more regular than the distance between them, then any correlation which is produced mainly by the distribution of velocities in a single jet will be less 'smeared out' than one depending on having the probes in different jets. The asymmetry of the negative regions is thus quite understandable and these general comments

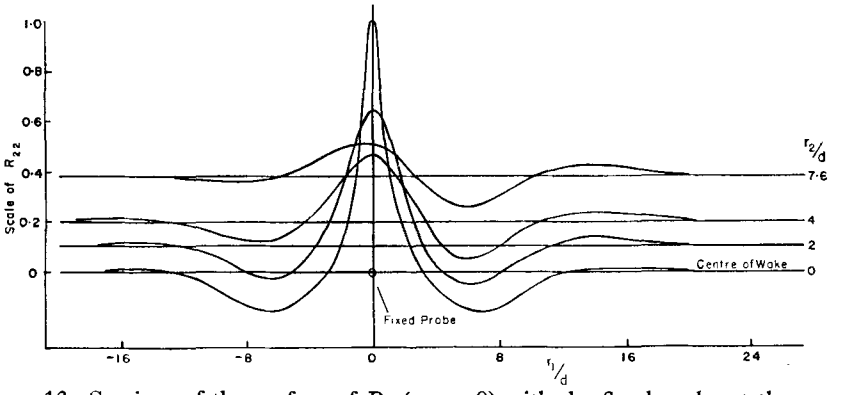


Figure 13. Sections of the surface of $R_{22}(r_1, r_2, 0)$ with the fixed probe at the centre of the wake.

would seem to apply to the outer positive regions as well but I am not able to offer any explanation of the asymmetry of the positive regions in terms of the detailed structure. Figure 13 shows the $R_{22}$ correlation with the fixed wire at the centre of the wake. The positive peaks become asymmetrical when the movable wire is only a short distance from the wake centre, which indicates that they cannot be accounted for by the inward velocity at B (figure 12) which is a rolling-up of the end of the tongue of turbulent fluid and does not extend into the core of the wake.

This model also suggests an explanation for the minimum in $R_{11}$ along the line $x$ = constant which passes through the fixed wire (figure 8). The large scale irrotational motions whose shapes are indicated roughly by dashed lines in figure 12 will contribute negative values of $R_{11}$ with the fixed wire at the outside of the wake and the other at the wake centre. When the wires are at opposite sides of the wake and at the same value of $x$, then when one wire is at a place where the contribution to $u$ from the large

irrotational motion is a maximum, the other is likely to be in a place where it is nearly zero. Upstream and downstream of this last wire, positive contributions to $u$ will be found. This situation would lead to negative values of $R_{11}$ at this point but a positive contribution to the correlation is expected from the vortex pair eddies so that the observed values of $R_{11}$ are qualitatively consistent with the assumed structure.

The correlation $R_{22}$ has a positive peak along the line $x$ = constant, $z$ = constant, which passes through the fixed wire (figure 10). For values of $r_2$ less than half the wake width, this may be attributed to small scale disorganized eddies but when the two wires are on opposite sides of the wake, it requires that the location of the jets on opposite sides of the wake should be correlated but sufficiently out of phase to produce positive values of $R_{22}$. The jets in figure 12 show the relationship that is envisaged and is commonly observed in the water tank experiments.

### 3.4. *The origin and maintenance of the vortex pair eddies*

The correlation $R_{33}(0, 0, r)$ has been selected as the single correlation that is most representative of the vortex pair eddies, i.e. the one that seems most unlikely to arise from some other kind of eddy. This has been measured for values of $y$ near the point of maximum shear at 250 and 533 diameters from the $\frac{1}{8}$-in. cylinder and at 546 and 1075 diameters from the $\frac{1}{16}$-in.

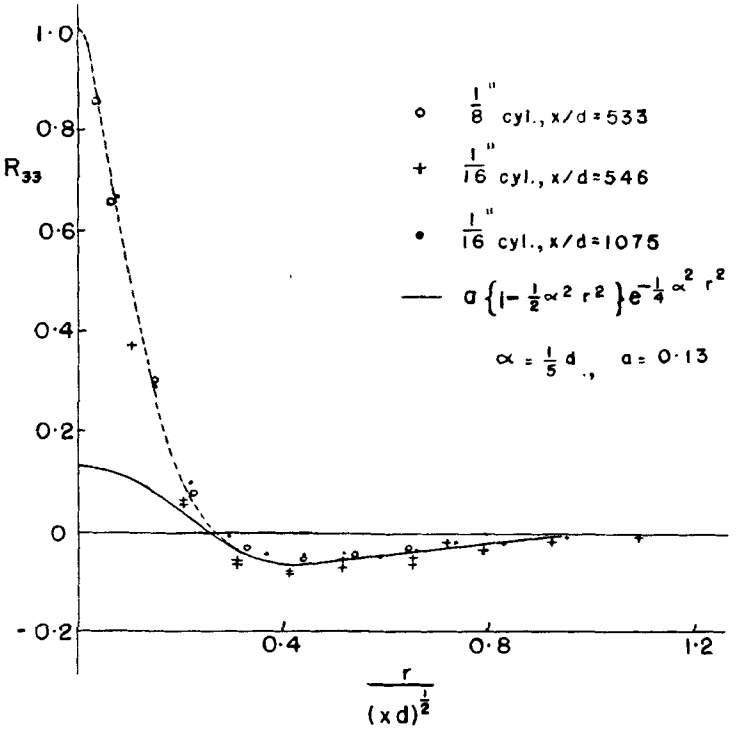


Figure 14. $R_{33}(0, 0, r)$ at different distances from the cylinder.

cylinder. In all cases, $U = 625$ cm/sec. The results are plotted in figure 14 and indicate a self-preserving increase of scale after 500 diameters at about the same rate as the increase of the mean velocity scale.

It has been assumed that these eddies contain no $v$ component of velocity. This is supported by evidence from the nine covariance components (figure 2). $R_{22}(0, 0, r)$ is always positive so that any $v$ component other than a translational velocity of the whole eddy must come through a tilt of the axes of rotation in the $(y, z)$-plane. Even if this occurs, it is not of much interest since a tilt in that direction does not put the eddy in a position to gain energy through stretching by the mean shear. It appears likely that these eddies have been initially formed in the neighbourhood of the cylinder and are merely decaying with time. A determination of $R_{33}$ in the $(x, z)$-plane has been made with the fixed wire at a distance of 2 in. (16 diameters) behind the $\frac{1}{8}$-in. cylinder. The result is shown in figure 15.

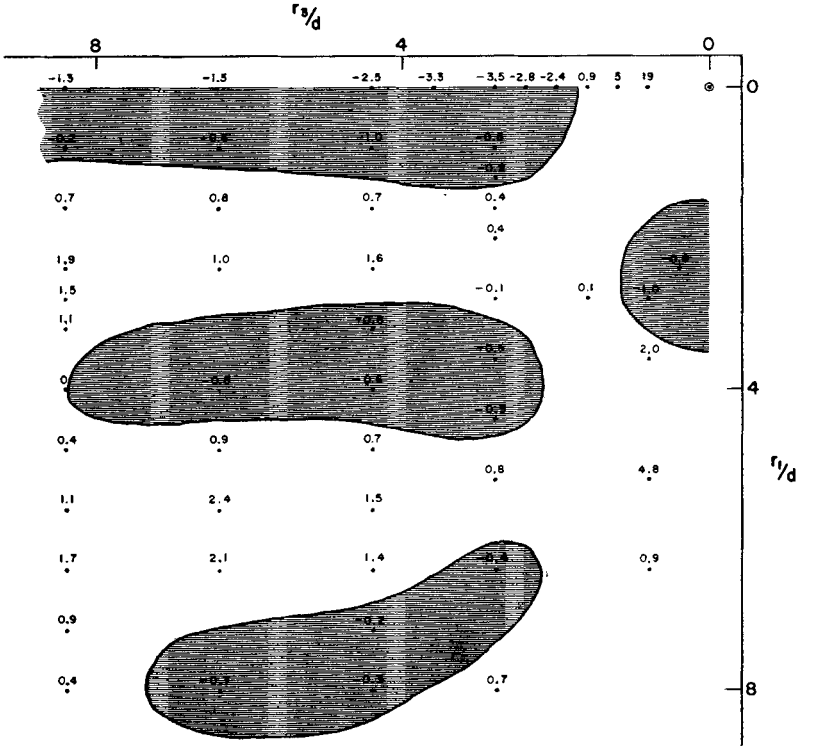


Figure 15. Contours of zero correlation for $R_{33}(r_1, 0, r_3)$ with the fixed probe at $x/d = 16$. Correlations expressed as percentages.

This plot has many of the characteristics of the corresponding one at 533 diameters (figure 6). Here, however, there is a periodicity in the $x$-direction, patches of negative and positive correlation alternating with the Kármán street frequency. This probably represents a folding of the Kármán eddies as they break up.

There is some evidence that, when these eddies are destroyed, the first thing that occurs is the development of waves in the long vortices. Roshko (1954) found a periodicity in the $R_{11}(0,0,r)$ correlation in the Kármán street region behind a cylinder at Reynolds numbers over 500, and Hamma, Long & Hegarty (1957) have described a similar structure in the transition of a boundary layer. They towed through still water a flat plate with a small cylinder attached spanwise about 30 cm from the leading edge. They found that long vortices were regularly shed from the cylinder and that, at a high enough Reynolds number, these vortices quickly developed periodic waves in the $(x,z)$-direction. The plane of the waves then rotated so that the downstream maxima were carried away from the plate and the stretching of the vortex lines in the velocity gradient resulted in an amplification of the periodic disturbance leading to 'horse-shoe vortices'. If a similar thing happens in the wake of a single cylinder, one might expect to find that the break-up of the street would leave the remains of horse-shoe vortices oriented in assorted directions—especially if the rotation of the wavy vortex carries some of it into the opposite side of the wake.

There are other conceivable mechanisms but any folding or faulting can produce pairs of eddies rotating in opposite directions and it is probable that any eddy whose plane of circulation is not very nearly the $(x,z)$-plane will be quickly stretched out by the mean flow gradient and destroyed. Those whose orientation is right may at this time go through the energy gaining stage proposed by Townsend but eventually they will be destroyed. A pair of eddies suddenly thrust into position with their axes normal to the plane of the wake and planes of circulation in the $(x,z)$-plane may at this stage have its middle torn out by the mean velocity gradient, but later, as the gradients are reduced, it may re-establish itself across the wake. It thus seems possible that the eddies with which we are concerned are simply selected bits of the Kármán street.

I tried to verify this idea by producing a wake which began without periodicity but I was unable to make such a wake. The bodies whose wakes were investigated were flat plates with holes or roughness to produce a turbulent boundary layer on the body. In all cases a large periodic component was found in the turbulence behind the trailing edge and the correlation $R_{33}(0,0,r)$ was found to be negative at large $r$.

Having failed to produce a wake without vortex pair eddies, I investigated the persistence of these eddies in a flow with no transverse mean velocity gradient. A grid of parallel cylinders of diameter 0·052 in. and spacing 0·30 in. was used for this purpose. It is well known that the mean velocity variation disappears within about 30 mesh-lengths of such a grid which in this case is a distance of 10 in. The correlation $R_{33}(0,0,r)$ was measured at distances of 477 and 1010 cylinder diameters downstream of this grid and the result is shown in figure 16. The correlation is negative at large values of $r$ and is self-preserving when plotted as a function of $(xd)^{1/2}$. The solid line on the figure is the self-preserving curve for $R_{33}(0,0,r)$ in the wake of a single cylinder and it coincides with the grid observations

at large values of $r$. It is to be expected that there will be differences at smaller values of $r$ because there is now a larger characteristic length in the problem (the mesh-length) and much of the energy of the original mean flow variation must have gone into turbulence with length scales of this order. This suggests that this turbulence, which has no mean velocity variation, contains vortex pair eddies which are the same size and growing at the same rate as those in the wake of a single circular cylinder. If that is so, the vortex pair eddies are probably formed near the cylinder and the mean velocity gradient must play no part in their development. The streamlines of the eddies must then be parallel to the $(x, z)$-plane.

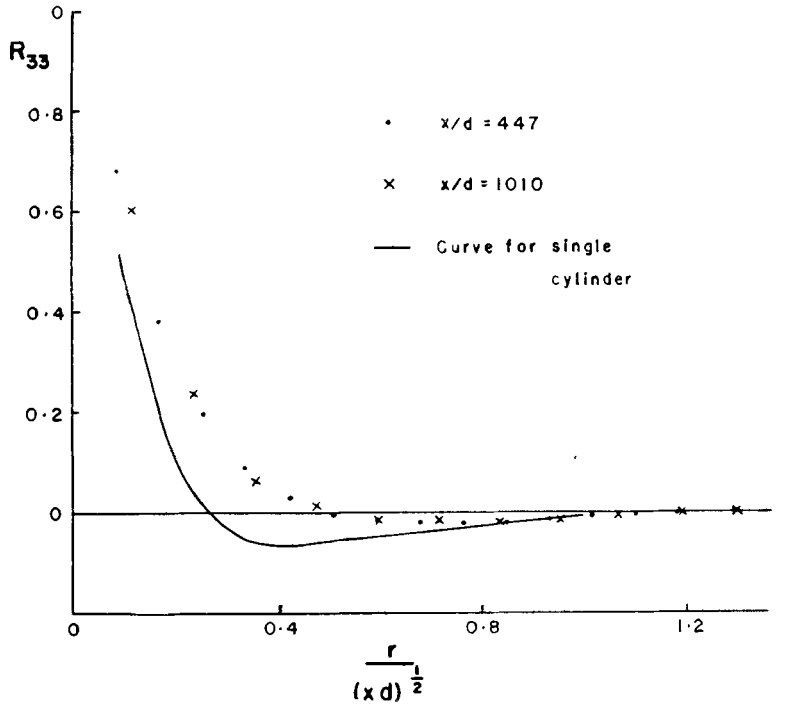


Figure 16. Comparison of $R_{33}(0, 0, r)$ in the wake of a parallel cylinder grid with that in the wake of a single cylinder.

Unfortunately, this argument does not satisfactorily account for the shape of the eddy in the $(x, y)$-plane that is suggested by the values of $R_{33}$ (figure 6). With respect to a point near the outer edge of the wake, the centre is only retarded by a distance of 3·3 cm at 500 diameters downstream from the cylinder. The mean velocity distribution is known over most of the wake (Townsend 1956, pp. 140–2) and it can easily be shown that an eddy with its axis straight and in the $y$-direction at $x/d = 30$ should have its centre retarded by about 10 cm at $x/d = 500$. This might be partly accounted for by the presence of more disorganized turbulence of comparable

scale in the $(x, y)$-plane. The effect could hardly be great enough to account for the whole discrepancy, however, and it is not yet safe to conclude that the vortex pair eddies all originate near the cylinder, although it is hard to escape that conclusion in the case of the parallel cylinder grid. This question will be considered again after the details of the mixing jets have been discussed.

### 3.5. *The mechanism of the mixing jets*

When a non-turbulent viscous fluid is subjected to a strain there are stresses set up in the fluid which are in many ways similar to those in an elastic solid but with the difference that the stress is proportional not to the strain but to the rate of strain. There is, therefore, no energy of deformation and when the rate of strain becomes zero there is no tendency for the fluid to return to its original configuration. The work done on the fluid has gone into heat and perhaps a change of pressure.

When a turbulent fluid is strained, the situation is somewhat different. The viscous forces extract energy directly from the mean flow in the same way but there is an additional stress resulting from the presence of the turbulence. This has commonly been considered to have the same character as a viscous stress and it is accounted for in the mixing length theories by defining an additional viscosity known as the 'eddy viscosity'. This procedure has been recognized to be physically unsound (e.g. Townsend 1954, Stewart 1956) although in spite of that it is sometimes found convenient. For the present purpose, the important difference between the viscous stress and the turbulent stress is that work done against the latter goes not into heat but into the production of turbulent energy and that an important part of the process is a redistrbution of energy among the turbulent velocity components which results in something very like the energy of deformation in an elastic solid.

In general, the process by which the turbulence gains energy at the expense of the mean velocity gradient is not well understood. Batchelor & Proudman (1954) have made a theoretical analysis of the effect on a turbulent field of an instantaneous finite plane strain and they have given expressions for change of energy of the different components of turbulent velocity. The first-order effect is simply a redistribution of energy among the turbulent velocity components to provide an increased intensity of the component in the direction of the compression and a decreased intensity of the component in the direction of the extension. The second-order terms show an increase in the total energy which is shared, although not equally, by all the velocity components. This is an extremely simple situation and the effect of a finite and prolonged rate of strain on turbulence which is neither isotropic nor homogeneous is bound to be more complicated. It is to be expected, however, that there will be a large effect similar to the redistribution of energy described above as it is essentially an increase of

velocities associated with vorticity aligned in the direction of stretch and a decrease of velocities associated with vorticity in the direction of compression.

In a plane wake, the nature of the strain is a combination of a rotation and a plane strain with principal axes of strain in directions at 45° to the usual coordinates. The resultant anisotropy of turbulent intensity is also greatest for axes aligned approximately in these directions. The subscript $s$ will be used to indicate velocities and directions in a coordinate system based on the principal axes of strain, the relation to the usual coordinates is indicated in figure 17 for one-half of the wake. The relation between the velocities is given by

$$u_s = \frac{u-v}{\sqrt{2}} \quad \text{and} \quad v_s = \frac{u+v}{\sqrt{2}}.$$

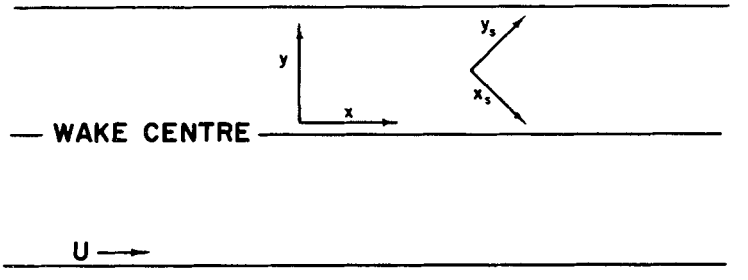


Figure 17. Relation between the ordinary coordinate system and the one aligned with the principle directions of strain for one half of the wake.

The degree of anisotropy can conveniently be expressed by the quantity

$$K_1 = \frac{\overline{u_s^2} - \overline{v_s^2}}{\overline{u_s^2} + \overline{v_s^2}},$$

and Townsend has measured the closely allied quantity

$$-\frac{\overline{uv}}{\overline{u^2}} = \frac{\overline{u_s^2} - \overline{v_s^2}}{2\overline{u_s^2}},$$

which he calls the shear coefficient. He finds that in the fully turbulent part of the wake, not too near the centre, the shear coefficient is nearly independent of $x$ and $y$ and has a value of about 0·4. To explain this, he postulated a 'structural equilibrium' in which an increase of anisotropy was opposed by a relative change in the rates of transport of energy along the spectra of the two velocity components. This proposal has not been entirely satisfactory, particularly in the other situation where it has been used (see § 5.2) and a different explanation of the constancy of the shear coefficient is attempted below.

When the equations of mean motion are expressed with respect to the principal axes of stress, only the normal components of the Reynolds stress are non-zero and for a shear flow in a steady state we have

$$U_s\frac{\partial U_s}{\partial x_s}+V_s\frac{\partial U_s}{\partial y_s}+\frac{1}{\rho}\frac{\partial \bar{P}}{\partial x_s}+\frac{\partial \overline{u_s^2}}{\partial x_s}-\nu\left(\frac{\partial^2 U_s}{\partial x_s^2}+\frac{\partial^2 U_s}{\partial y_s^2}\right)=0,$$

$$U_s\frac{\partial V_s}{\partial x_s}+V_s\frac{\partial V_s}{\partial y_s}+\frac{1}{\rho}\frac{\partial \bar{P}}{\partial y_s}+\frac{\partial \overline{v_s^2}}{\partial y_s}-\nu\left(\frac{\partial^2 V_s}{\partial x_s^2}+\frac{\partial^2 V_s}{\partial y_s^2}\right)=0,$$

$$W=0.$$

Stewart (1956) has pointed out that the quantities $\rho\partial\overline{u_s^2}/\partial x_s$ and $\rho\partial\overline{v_s^2}/\partial y_s$ have the same effect as pressure gradients and that $\rho\overline{u_s^2}$ and $\rho\overline{v_s^2}$ are equivalent to the components of a pressure which in anisotropic turbulence are different in different directions. If the turbulence is homogeneous, these pressures are uniform and such a situation could be stable. On the other hand, an isolated blob of anisotropic turbulence in an irrotational fluid is clearly unstable. The pressures on its boundary will be large where the boundary is normal to the direction of high intensity and small where the boundary is normal to the direction of low intensity. The irrotational fluid can only respond with accelerations which will result in an extension of the blob in the direction of high intensity and a contraction in the direction of low intensity, which is the sense required to equalize the intensities.

The blob of anisotropic turbulence can be said to contain a stress acting in directions which tend to return it to the shape which it had before being strained if that was how the anisotropy was produced. There is a clear resemblance to the stress in an elastic solid but there are two important differences. One is that the stress is only meaningful if it involves averages over volumes large compared with the scale of the turbulence. The other is that to the first order, the energy available in the stress does not represent work done by the straining agent. It has arisen by a redistribution of turbulent energy and so may not bear much relation to the work done in straining the fluid.

The turbulence in a wake is under a continuous applied strain which is non-uniform and of different sign in opposite sides of the wake and it is bounded on both sides by irrotational fluid which is not being strained. That the anisotropy does not increase indefinitely is shown by Townsend's measurements of the shear coefficient, so the turbulent stress must be released by some means. This could conceivably come about through an unequal rate of transfer of energy along the spectrum in the two velocity components or through the medium of secondary flows similar to those expected about the isolated blob of strained turbulence which was discussed above. It is probable that both mechanisms operate to some extent and the mixing jets seem to be the result of stress relief by secondary flows.

If the bounding surfaces of the wake were plane on a scale an order of magnitude larger than the turbulence, the stress might be in equilibrium

because the resultant force would be everywhere in the same direction across the boundary. The situation would probably be unstable, however, and we can make a guess about the physical nature of the flow resulting from the instability. If there is a bump on the bounding surface, and the turbulence in the wake has been uniformly strained, the pressure acting across the surface on one side of the bump will be different from that on the other. The irrotational fluid can only see this as a high pressure region and a low pressure region and fluid will begin to flow from one side of the bump to the other. The type of flow that is envisaged is illustrated in figure 18 (*a*). This might be expected to lead to a jet similar to those

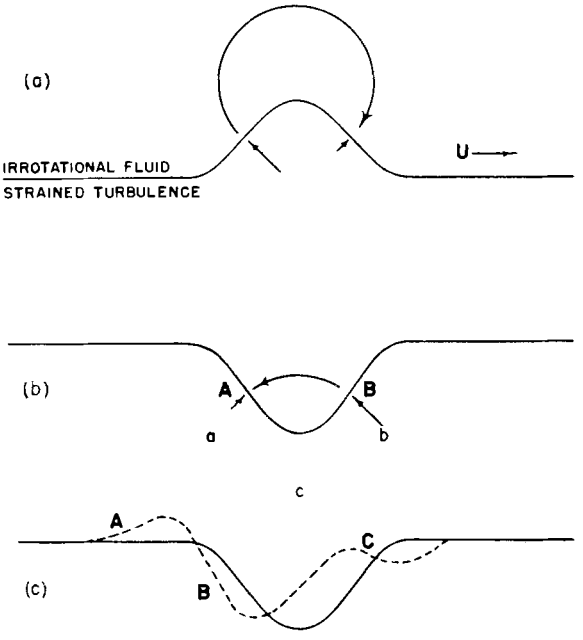


Figure 18. The effects of distortion of a boundary between stressed and unstressed fluid.

which have been observed. It might appear that a hollow in the turbulent fluid would induce a jet which bends in the opposite direction, but this is probably not so. Consider figure 18 (*b*). If a flow is set up from *B* to *A* in the irrotational fluid so that the flow in the turbulent fluid is simply a reflection of the turbulent jet, i.e. a jet of laminar fluid entering at *A*, then the fluid in the region *a* would have to expand in the direction *a*–*c*, which would always be up the gradient of normal turbulent pressure because an irrotational inflow from *a* and an outflow to *b* would serve to increase the stress at *c*. It would thus seem more likely that the expansion at *a* would be in the outward direction and contraction at *b* from the outer side. This would lead to a boundary like the dashed line in figure 18 (*c*) before the stress had been much reduced. We now have two bumps and

flow in the irrotational fluid from $A$ to $C$ or from $A$ to $B$ would be in a direction to relieve the stress deep in the fluid.

Even if the flow in the outer fluid in figure 18 ($c$) is from $A$ to $B$, there is still an inclined surface to the right of $B$ which could be the source of another jet and the jet arising from a single bump will also quickly cause a similar depression of the surface of the in-going side. It would seem that a roughly periodic set of jets might be expected to occur when a single one is started and this periodicity can be seen both in the photographs and the correlations (figures 10, 11). In the water tank it was common to see a set of from three to five jets on one side of a wake, all of approximately the same size and arranged approximately periodically. At a later stage, a new and larger set would arise in the same region of the wake.

The boundary of a wake is never as simple as this model but it should be noted that in a fully developed wake, the boundary that matters is not the boundary of turbulent fluid but the boundary of stressed fluid. Although the outer part of a wake is very ragged after a series of jets has spent itself, the boundary of newly-stressed fluid may be quite regular, although diffuse, and some time may elapse before a suitable distortion of the 'surface' occurs to set off another series of jets.

As the fluid is strained, the jets probably do not appear at any particular value of the stress, their initiation depending more on a chance configuration of the boundary. From observation of the wakes in water, I have formed the opinion that there is an irregular variation of the velocities and extent of travel of successive sets of jets. The scale, however, appears to increase more regularly. Very soon after a jet begins, its effects probably reach right in to the centre of the wake and it is this length scale, the half-width of the mean velocity distribution, which probably determines the scale of the jets. The variation of $R_{22}$ over the $(x, y)$-plane was determined at $x/d = 274$. The ratio of the 'wavelength' to that at $x/d = 533$ (figure 10) was found to be the same as the ratio of the widths of the mean velocity distribution at these two points (Townsend 1956, fig. 7.1).

If we consider both sides of the wake together, it can be seen that their stress relieving action is not entirely independent. Referring to figure 19, a jet affecting the region $A$ may draw fluid from the region $B$ in the opposite side of the wake. This would be expected to disturb the boundary of stressed fluid on the $B$ side of the wake and produce a jet there as shown. It has been observed in the water tank that jets on one side of the wake are commonly accompanied by jets on the other side with their roots displaced slightly in the $x$-direction.

The equilibrium value of the shear stress is probably an average over all stages of the build-up and release of stress. Why it takes the particular value it does, cannot be fully understood without an analytical treatment of the instability, but it probably depends on the average time required for a suitable perturbation of the boundary to occur. This model requires that the local value of the shear stress should vary in time and space, taking values ranging from near zero to something larger than the measured

average value. Evidence for this might be found in the probability distribution of the turbulent velocity components in the directions of the principal axes of stress. Townsend (1956, pp. 153–4) has obtained values of the flatness factor of the distribution of $u_s$ and $v_s$. At a point away from the centre of the wake but not so far out that the intermittency is important, he finds that the flatness factors of $u_s$ and $v_s$ are 2·6 and 3·6 respectively. In the same region the flatness factors of $u$, $v$ and $w$ are very nearly 3·0 which is the value for a normal distribution (Townsend 1948).

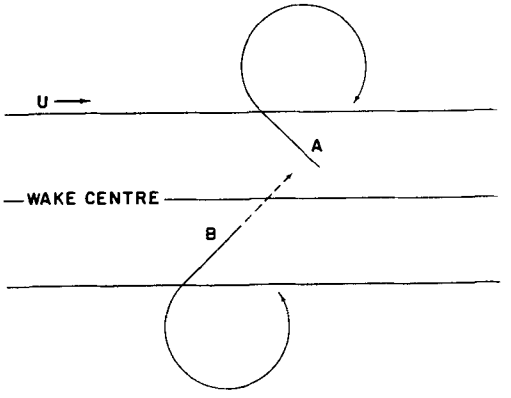


Figure 19. The relation between jets on opposite sides of the wake.

This information by itself is not very useful but it does indicate that the distribution does not consist of patches of stressed and unstressed fluid. If that were the case, higher values of the flatness factor would be expected. The observed values are not inconsistent with the idea that the frequency distribution of velocities is derived from a field which contains a wide but continuous range of values of the stress.

### 3.6. *The rate of strain*

As the mean velocity distribution shows, there is a finite mean rate of strain over much of the wake and it is not changing very rapidly with distance from the cylinder. The mechanism for releasing the excess stress must therefore operate without removing all the strain and without transferring it all to the outside of the wake. There are at least two reasons why the total strain is not removed with the accumulated stress. One of these is that the rotational part of the applied strain serves to rotate the principal directions of stress with respect to the principal directions of strain. This rotation might be as much as 15°. The other reason is that any stressed fluid carried into the opposite side of the wake becomes fluid of negative stress in its new surroundings. This fluid can then suffer some positive strain without building up any positive stress. We must also admit the possibility that some stress disappears through unequal rates of transfer of energy along the spectra of the different velocity components. It is not possible to estimate the magnitude of these effects quantitatively because the geometry of the

stress releasing motions is not known well enough. There must certainly be some loss of total strain the in process so that, within a series of mixing jets, the downstream velocity near the centre of the wake is greater than the local mean velocity and the velocity outside the plane of maximum shear is less than the local mean velocity. As the jets die, these velocities on both sides of the plane of maximum shear will, on the average, approach the mean for the local values of $(x, y)$ because of the drag of the fluid on either side of the region occupied by the jets. When averaged over the cycle of build-up and release of stress, the rate of strain within the region occupied by the jets is less than that which is indicated by the mean velocity gradient and the effect will appear in the mean velocity distribution as a gradual reduction of the gradients with increasing $x$. At the exteme edge of the wake, the immediate effect is an increase of the mean velocity gradient which, on decay, will produce an increase in the width of the mean velocity distribution.

### 3.7. *Relation between the vortex pair eddies and the mixing jets*

The form of the vortex pair eddies has been quite well established but the evidence regarding their origin and their relation to the mixing jets is somewhat conflicting. They seem to exist in the wake of the parallel cylinder grid, which has no mean velocity gradient. It is hard to see how such a highly ordered structure could arise within the turbulence by the action of the non-linear terms of the Navier–Stokes equations, so it would seem that they must, in this case at least, have been formed near the cylinder. The objection to this is that in the wake of a single cylinder, where the structure can be seen more clearly, the centre of the eddy does not appear to be retarded enough to have experienced the mean shear for the whole time required to pass from near the cylinder to the point of observation.

It is possible that the phenomenon occurring in the cylinder wake is different from that in the wake of the grid. On this supposition, one could argue that the vortex pair eddies arise in the wake in its fully developed state. The likely mechanism would be that the eddies form about a tongue of fast irrotational fluid which is drawn into the wake as a part of the mixing jet action. There is, however, no sign of vortex pair eddies in the outer part of the turbulent boundary layer.

There is not enough evidence to resolve the problem with certainty but I think it most likely that these eddies do arise in the region of the vortex street. The reason for the small retardation of the centres of the eddies may be that they have a tendency to set off a mixing jet. If they have such a tendency, they will, on the average, be found superimposed on weak jets which appear before the stress vector has rotated much with respect to the strain. They would then have less than the average mean velocity gradient and would also be more likely to survive in a coherent form than if they were subject to some of the very large jets which draw irrotational fluid almost into the centre of the water wakes.

## 4. The turbulent boundary layer

### 4.1. *Correlations in the boundary layer*

Although the study of the large scale structure of the wake has been described first, the measurements were actually made after a similar but less extensive series in a turbulent boundary layer. The boundary layer experiments were not designed in the light of the experience with the wake, which is a simpler flow, but can be profitably discussed that way.

The wind-tunnel has been described briefly in § 2.3. The observations were made at a distance of 80 in. from the trip fence, and the mean velocity profile at that point is given in figure 20. The total thickness is about

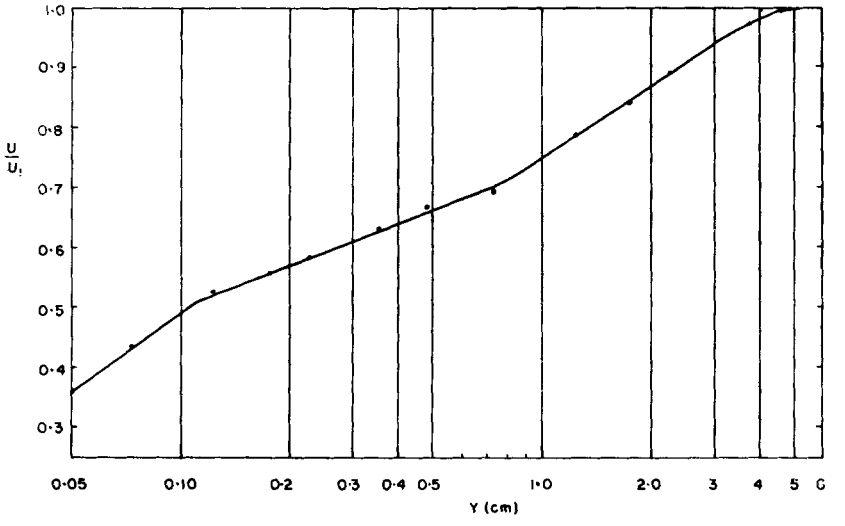


Figure 20. Mean velocity profile in the turbulent boundary layer.

5·5 cm and the thickness $\delta_0$, which is the distance from the wall to the point at which $U_1 - U = U_\tau$, is 3·8 cm ($U$ = mean velocity, $U_1$ = free stream velocity, and $U_\tau^2$ = wall stress/fluid density). The wall stress has been determined from the slope of the logarithmic part of the curve on the assumption that it is represented by

$$U = \frac{U_\tau}{K}\left[\log \frac{U_\tau y}{\nu} + A\right]$$

and that $K = 0{\cdot}41$ (Townsend 1956, p. 242). This profile agrees very well with most published 'flat plate' boundary layer profiles when plotted in the form $(U_1 - U)/U_\tau$ *vs* $y/\delta_0$. For example, it is in agreement over the whole layer with those collected by Townsend (1956, pp. 244–5).

The nine correlations are given in figure 21. These curves differ considerably from the corresponding ones for the wake. Perhaps the most noticeable thing is the large decrease in most of the length scales as the fixed probe moves nearer the wall. Because of this it is best to consider

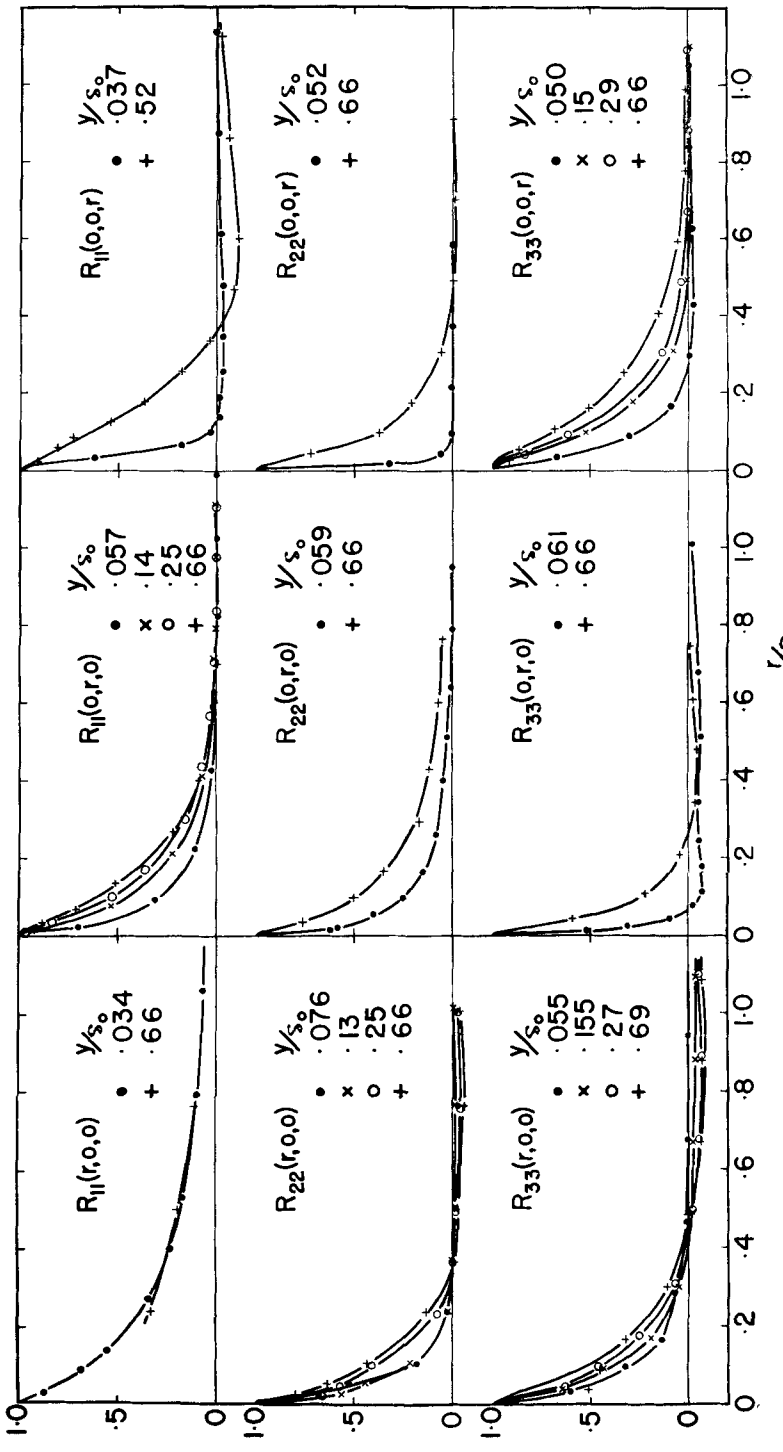


Figure 21. The nine correlations in the boundary layer.

the correlations in the outer part of the layer separately from those near the wall.

4.2. *The observations in the outer part of the layer*

The observations in the outer part of the layer are collected together in figure 22. Most of them are taken with the fixed wire at $y/\delta_0 = 0{\cdot}66$ which is near enough to the wall for there to be not much intermittency. The curves approach zero over a considerable range of values of $r$, indicating a wide range of length scales for different combinations of velocity component and direction of separation in the largest eddies. The correlations for the $w$ component are highly anisotropic even at small values of $r$.

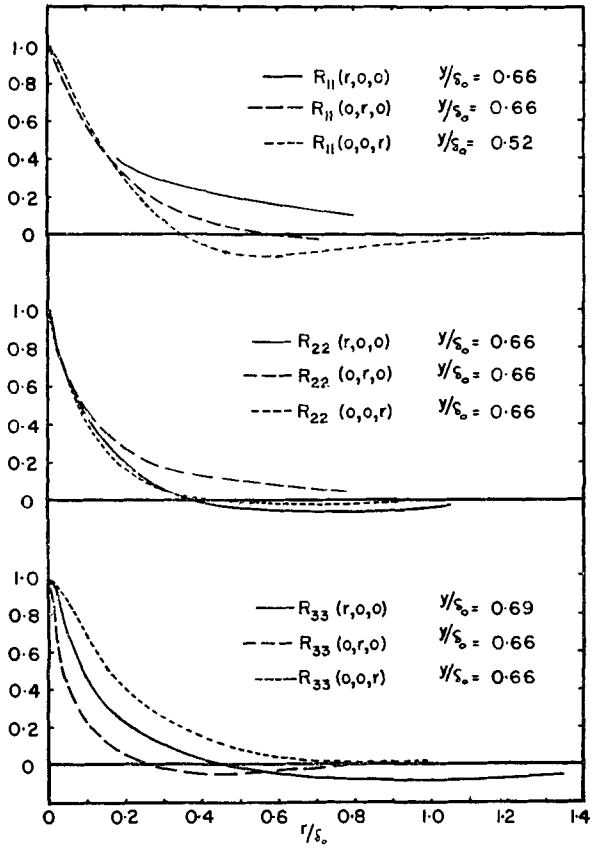


Figure 22. The correlations in the outer part of the layer.

The backflow corresponding to the different velocity components at the fixed probe can be located roughly. The curves for $R_{11}(0, r, 0)$ and $R_{11}(0, 0, r)$ show the $R_{11}$ correlation along two lines in the plane normal to the $u$ component of velocity. It can be seen that the back-flow contributed by the largest eddies takes place mostly at values of $r$ in the $z$-direction.

Similarly, for the $v$ component it occurs mostly in the $x$-direction and for the $w$ component in both the $x$- and $y$-directions although at different values of $r$.

It is tempting to try to use these back-flows individually or in pairs to infer the nature of the large motions. Not much can be done, however, beyond statements that certain simple large circulations are not dominant. As in the wake, the trouble is that even the nine correlations are only a small part of the specifications of the motion and cannot be expected to yield a unique solution without the aid of further evidence or hypotheses.

Although these correlations are quite different from the corresponding ones in the wake, their complication again indicates a considerable amount of order among the big eddies, and it is worth searching first for a set of large eddies of a single kind which will yield all the nine correlations at large $r$. Townsend's large eddy structure will produce the observed values of $R_{11}(0, r, 0)$ and $R_{11}(0, 0, r)$ quite reasonably but since the directions of the velocities in these eddies are independent of $x$, they cannot yield negative values of $R_{22}(r, 0, 0)$ and $R_{33}(r, 0, 0)$ even if they are reduced to finite length. They cannot therefore be used as a detailed picture of the large scale motion.

There is no suggestion of vortex pair eddies, notably because $R_{33}(0, 0, r)$ is clearly positive at all values of $r$. A number of other kinds of simple eddy were considered but there is not enough evidence to support any of them as a dominant structure.

The possibility of mixing jets similar to those observed in the wake would seem a likely one and most of the signs are there. $R_{22}(0, 0, r)$ goes very slightly negative this time but the negative values are so small that the character of the curve bears a clear resemblance to the corresponding one in the wake. $R_{22}(r, 0, 0)$ takes negative values as large as 5% but there is no sign of a periodicity here. $R_{11}(0, r, 0)$ is positive except for one point, out where the intensity is very low. $R_{22}(0, r, 0)$ is always distinctively positive as in the wake.

All the relevant components are thus consistent with the mixing jet idea except for the lack of periodicity in $R_{22}(r, 0, 0)$. A measurement of $R_{22}$ over the $(x, y)$-plane is given in figure 23. The fixed wire was at a distance $\delta_0$ from the wall and the other wire was moved along three lines between the fixed wire and the wall. The sections of the correlation surface have an asymmetry very much like that of the corresponding correlation in the wake (figure 10). There is no periodicity, but the curves have long flat negative tails which suggest motions with a wide range of sizes.

The extremely large rates of shear and the presence of the wall produce turbulence of a very small scale in the inner part of the boundary layer and since this scale is very much smaller than the thickness of the layer, it is likely that the turbulence undergoes stress releasing motions in this region which, although large compared with the local turbulence scale, are still small compared with $\delta_0$. Some of these will appear in the outer layer and the stress releasing motions will have quite a broad spectrum there.

Klebanoff (1955) has measured energy spectra in a boundary layer, and, except very far out in the intermittent region ($y/\delta_0 = 1{\cdot}5$), he found no peak in the spectrum. This is in contrast with the clearly defined two-component structure found by Townsend (1950) in the wake spectra. The asymmetry of figure 23 indicates that the individual motions have a character similar to those in the wake, i.e. they go in the same direction. The type of instability involved is about the same as in the wake but the part of the unstressed fluid in that model is often played in the boundary layer by fluid with smaller stress and this leads to a much more confused motion.

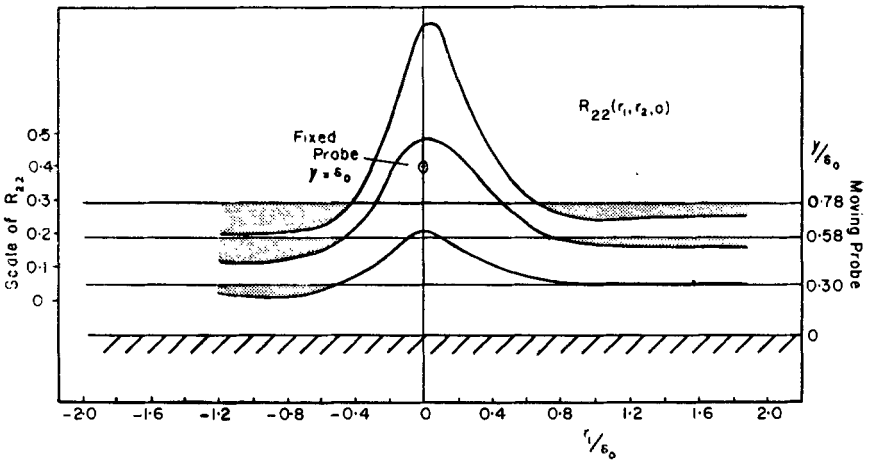


Figure 23. Sections of the surface of $R_{22}(r_1, r_2, 0)$ with the fixed probe at $y = \delta_0$.

4.3. *The motion near the wall*

Figure 24 shows the nine correlations at points near the wall but in the logarithmic region of the mean velocity curve. The distance from the wall varies between $0{\cdot}034\delta_0$ and $0{\cdot}076\delta_0$. A representative value would be $0{\cdot}055$. Comparison with figure 22 shows large differences both in scale and character.

There is no support here for the suggestion that the dominant form of the energy containing motions is the 'attached eddy'. The very great extent of $R_{11}(r, 0, 0)$ compared with $R_{22}(r, 0, 0)$ and $R_{33}(r, 0, 0)$ does not seem consistent with a simple eddy as we have used the term. The very small extent of $R_{22}(0, 0, r)$ strengthens this view.

These observations are consistent with the presence of stress releasing motions similar to those proposed for the outer part of the layer. The scale of these motions would be small compared with those originating in the outer part of the layer but large compared with the scale of the turbulence that contains most of the energy locally. If a series of jets of this size occur, lined up in the direction of the stream, then, because of the large velocity gradient, there will be a large contribution to the $u$ component of turbulent velocity. This contribution will be a function of $y$ but will

be nearly independent of $x$ over the whole length of the series of jets. Such a structure could produce positive values of $R_{11}(r, 0, 0)$ at values of $r_1$ many times the distance from the wall.

This picture is supported by several of the other correlations. The back-flow corresponding to the $u$ component of velocity at the fixed point occurs only in the $z$-direction, at least as far as the bigger scales are concerned. This implies stress relieving motions originating very near the wall, perhaps involving the boundary of the laminar sublayer. The motion would be in the nature of an outward eruption originating near the wall.

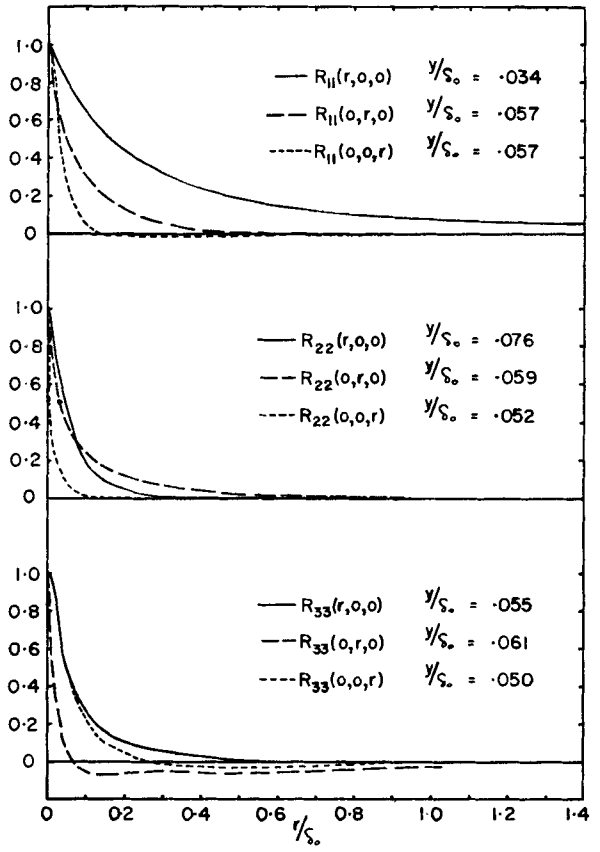


Figure 24. The correlations with the fixed probe near the wall.

The extremely short extent of $R_{22}(0, 0, r)$ means that the series of motions giving rise to the extended correlations in the $x$-direction is quite narrow in the $z$-direction, and its movement in the $y$-direction is not compensated by an opposite movement or even an extended drift in the region to the side of the occurrence. Rather, the back-flow appears to be in the $x$-direction, which would be expected in a stress releasing motion or a sequence of them lined up in the $x$-direction.

The negative values of $R_{33}(0,0,r)$ would then represent flow toward the displaced fluid on both sides because, very near the wall, rotational motions involving the $w$ component of velocity might take the place of the irrotational flow from the other side which was postulated in the wake. The back-flow for the $w$ component occurs only in the $y$-direction, which again suggests that the displaced fluid is long in the $x$-direction. When the fixed probe is moved a short distance away from the wall, $R_{33}(r,0,0)$ does become negative (figure 21), indicating a loss of order in the large scales of the $w$ component. Slightly further out, at about $y = 0{\cdot}25\delta_0$, $R_{33}(0,0,r)$ ceases to be negative. Beyond this level, it may be assumed that the nature of what may be locally described as large scale motions, is essentially the same as that described for the wake but with stress releasing motions of assorted size originating over a considerable range of values of $y$.

This description of the motion near the wall is supported by photographs published by Einstein & Li (1956), showing coloured fluid from the laminar sublayer erupting into the turbulent fluid over a limited region of the wall. Unfortunately, the present experiments do not yield any information relevant to their proposal of an intermittent instability in the sublayer. The motions proposed here could be caused by the rapid production of shear stress which would occur just after a sudden transition in the sublayer. On the other hand, they might originate in the fully turbulent fluid but be vigorous enough to stir up part of the sublayer.

4.4. *Space–time correlations*

Some suggestions can now be made about the interpretation of the space–time correlations measured in a boundary layer by Favre, Gaviglio & Dumas (1957). The first of the two most outstanding points among their results is that for two probes separated in the $y$-direction, the time delay for maximum correlation increases, as the probe pair is moved downstream, at a faster rate than can be accounted for by the mean velocity gradient. The other is that, for one probe fixed and the other taking positions over the $(x,y)$-plane downstream, if values of $r_2$ and the time delay were adjusted for maximum correlation at each value of $r_1$, the locus of the points of maximum correlation was a curve which moved away from the wall much faster than a mean streamline.

The first of these observations is to be expected if the large scale motions in the boundary layer are essentially the same as those which have been found in the wake, except that there is nothing equivalent to the interaction between the two sides of the wake. That is, they consist of ' eddies ' always rotating in the same direction, which is such that on the outer side they are moving faster than the local mean velocity and on the wall side slower than the local mean velocity. The second observation indicates that (as has been assumed here) the outgoing part of the motion is more coherent than the ingoing part so that it can, when it is convenient, be thought of as a jet. The line of maximum correlation in time and space is thus something like an average streamline for particles within jets. The velocity of such particles

will, of course, be expected to maintain a non-zero correlation for much longer periods than particles not in jets.

## 5. Grid turbulence

### 5.1. *The large eddies of grid turbulence*

The presence of vortex pair eddies in the cylinder wake suggested that something similar might be found in grid turbulence which, at its origin, consists of a combination of cylinder wakes. Much of the experimental work on grid turbulence has been done with the assumption that, at some distance from the grid, the motion is an accurate approximation to theoretical isotropic turbulence. In the theoretical case, all nine correlations are determined by a single scalar function $f(r)$, which in the present notation is $R_{11}(r,0,0) = R_{22}(0,r,0) = R_{33}(0,0,r)$. The other six non-zero correlations have a single form $g(r)$, which is a function of $f(r)$ (Batchelor 1953). When this is assumed to be true, complete experimental information on the correlation tensor is obtained by determination of $f(r)$ in the form $R_{11}(r,0,0)$, but it is a simple matter to measure $g(r)$ directly using the downstream component of velocity and this has also been done (Stewart & Townsend 1951). It has been shown by Grant & Nisbet (1957) that the turbulence is not isotropic in the sense that $\overline{v^2} < \overline{u^2}$. The idea of isotropy with regard to the correlation components was thus in question and a direct test was desirable.

The coordinate directions which have been chosen for the grid are those of the trailing set of bars. If the vortex pair eddies are to be found here, they will presumably come from the wakes of each set, so a single correlation will be a combination of contributions from each set of vortex pair eddies. Table 1 gives the nine correlations in the grid notation, and the components which they include in the notation appropriate to the two different sets of wakes. Also given are the signs of these correlations at large $r$ and the sign that might be expected in the grid turbulence. The results of some measurements of $R_{22}(0,r,0)$, $R_{33}(0,0,r)$, $R_{22}(0,0,r)$ and $R_{33}(0,r,0)$ are given in figure 25 for a 1-in. grid at 80 mesh-lengths and a 2-in. grid at 30 mesh-lengths. In every case, the sign of the correlation at large $r$ is different from that which is expected in isotropic turbulence. It appears that the large scale motions retain some of the anisotropic characteristics of the original wakes for a very long time; probably throughout the life of the turbulence.

### 5.2. *The effect of a plane strain on the large motions of grid turbulence*

Some years ago, Townsend (1954) made a study of the effect of a plane strain on grid turbulence. He constructed a duct of constant cross-sectional area which, when placed downstream of a grid, compressed the turbulent fluid in one transverse direction and extended it in the other. He found that, in terms of coordinates aligned with the principal axes of strain, the

| Grid | Isotropic turbulence type | Wake of trailing bars | Wake of leading bars | Expected sign at large $r$ | Observations |
|---|---|---|---|---|---|
| $R_{11}(r, 0, 0)$ | $f(r)$ | $R_{11}(r, 0, 0)$ (+) | $R_{11}(r, 0, 0)$ (+) | + | Found positive by Townsend. |
| $R_{11}(0, r, 0)$ | $g(r)$ | $R_{11}(0, r, 0)$ (+) | $R_{11}(0, 0, r)$ (−) | ? | At least one of these observed to be negative. |
| $R_{11}(0, 0, r)$ | $g(r)$ | $R_{11}(0, 0, r)$ (−) | $R_{11}(0, r, 0)$ (+) | ? | (Stewart & Townsend 1951). |
| $R_{22}(r, 0, 0)$ | $g(r)$ | $R_{22}(r, 0, 0)$ (−) | $R_{33}(r, 0, 0)$ (−) | − | |
| $R_{22}(0, r, 0)$ | $f(r)$ | $R_{22}(0, r, 0)$ (+) | $R_{33}(0, 0, r)$ (−) | ? | Negative (figure 25). |
| $R_{22}(0, 0, r)$ | $g(r)$ | $R_{22}(0, 0, r)$ (+) | $R_{33}(0, r, 0)$ (−)* | + | Positive (figure 25). |
| $R_{33}(r, 0, 0)$ | $g(r)$ | $R_{33}(r, 0, 0)$ (−) | $R_{22}(r, 0, 0)$ (−) | − | |
| $R_{33}(0, r, 0)$ | $g(r)$ | $R_{33}(0, r, 0)$ (−)* | $R_{22}(0, 0, r)$ (+) | + | Positive (figure 25). |
| $R_{33}(0, 0, r)$ | $f(r)$ | $R_{33}(0, 0, r)$ (−) | $R_{22}(0, r, 0)$ (+) | ? | Negative (figure 25). |

Table 1. Sign of correlations at large values of $r$. The negative values of $R_{33}(0, r, 0)$ marked with an asterisk are assumed to be caused by the bend in the eddy; this effect should not be so pronounced in the grid turbulence where the mean velocity is uniform, hence the expected positive correlation.

structure parameter $K_1 = (\overline{v^2} - \overline{w^2})/(\overline{v^2} + \overline{w^2})$ became constant after a total strain ratio of about 2. The value of $K_1$ at this point was about 0·4, which is very close to the equilibrium value of the shear coefficient in the turbulent wake.

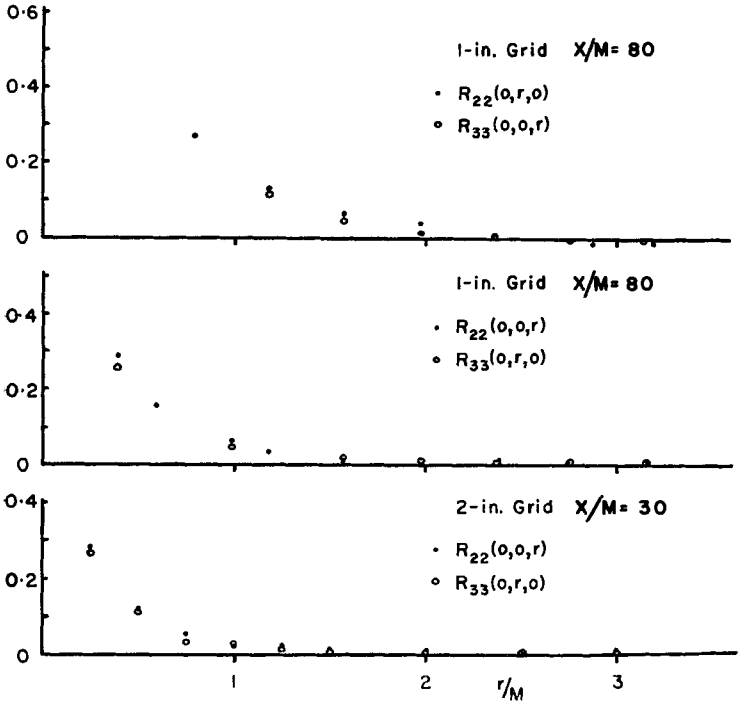


Figure 25. Correlations measured in grid turbulence.

Townsend suggested that the cause of the equilibrium is that the crowding together of the favoured eddies causes an increased rate of transfer of energy from these to smaller eddies. As he pointed out, the difficulty with this explanation is that when the distortion ceases, the anisotropy decreases only very slowly. This hypothesis would require that eddies of a given energy can be located relative to each other in such a way that the energy transfer is normal but if any energy is transferred from one component of turbulent velocity to the other, it is immediately passed on to more disordered turbulence.

I reconstructed the wind-tunnel with the distorted duct but with a longer parallel flow section after the distortion (figure 26). The coordinates used are those of the trailing set of bars in the grid which is oriented so that $y$ is in the direction of compression in the distorting section and $z$ is in the direction of extension. The origin of $x$ is at the grid. In this tunnel, I was able to measure $K_1$ at a distance of 26 in. after the end of the distortion. The turbulence was not very homogeneous but an average of seven readings at different points over the tunnel section was $K_1 = 0{\cdot}397$ with a standard

deviation of 0·024. There is no doubt that the anisotropy is decreasing only very slowly (figure 27).

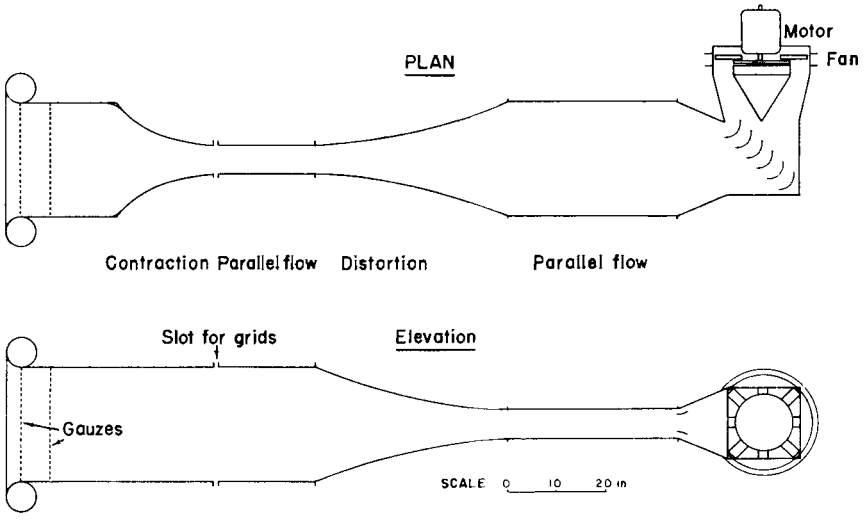


Figure 26. The wind tunnel with the distorting duct which applies a uniform plane strain to grid turbulence.

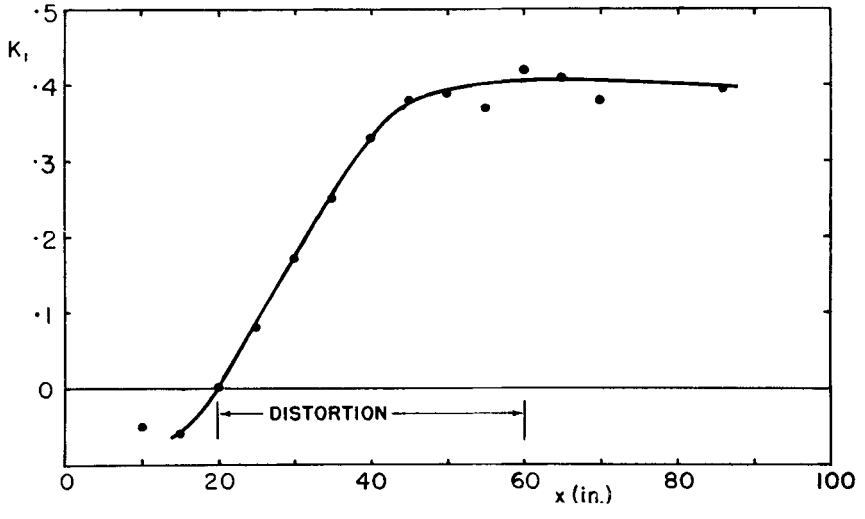


Figure 27. The structure parameter $K_1$. The point at $x = 86$ in. is the new one. The others were determined by Townsend (1954). $M = 1{\cdot}27$ cm, $U = 625$ cm/sec.

The similarity between the behaviour of $K_1$ in this flow and in the wake, suggests that the mechanism which maintains a constant average stress is similar in the two cases. It is hard to predict the form of the stress relief in detail, but it must occur in patches or cells and the typical motion would

be something like that described for a 'blob' of anisotropic turbulence in an irrotational fluid. If the turbulence were perfectly homogeneous, it might be in equilibrium even for large stresses, but in practice there is probably always enough variation of intensity to make an instability possible for some level of stress.

One thing that can be expected is that the stress relieving motions will be in the $(y,z)$-plane and be considerably larger than the typical scale of the turbulence. This should lead to negative values of $R_{22}(0,0,r)$ and $R_{33}(0,r,0)$ at large values of $r$. The result of a measurement of $R_{22}(0,0,r)$ at a point three inches before the end of the distortion is given in figure 28.

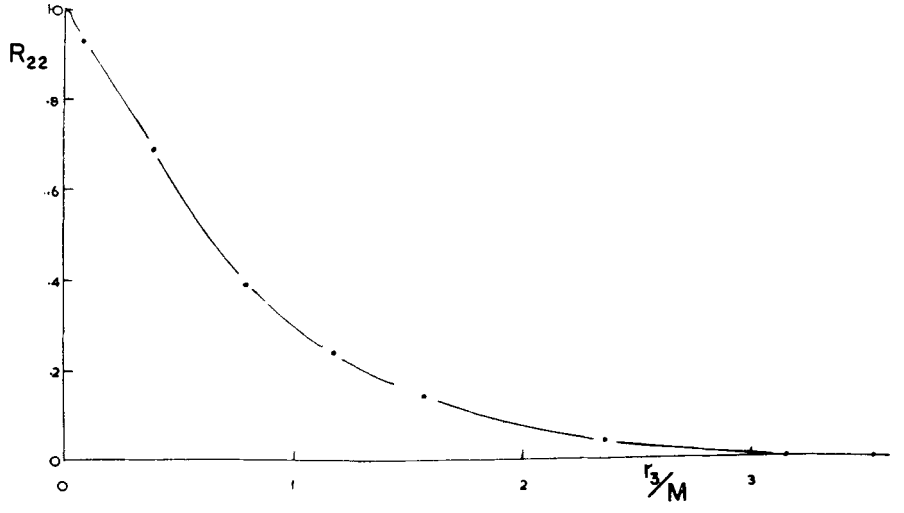


Figure 28. $R_{22}(0, 0, r)$ near the downstream end of the distorted duct. Fixed probe at $x = 57$ in.

This point was 154 mesh-lengths from the grid and, in the absence of a strain, we would expect a curve not much different from those shown in figure 25 (*b*). The scale has increased by more than a factor of two and there are no negative values. The increase of scale in this component is caused by the extension of eddies with vorticity in the $z$-direction and the stress releasing motions probably have a similar scale so that their negative contribution is masked by the effect of the long eddies.

The behaviour of $R_{33}(0,r,0)$ is more interesting. Figure 29 shows this correlation at several points in and after the distortion. Before the distortion this component is also positive at all values of $r$ but at $x = 39$ in., which is 19 in. after the beginning of the distortion, it is negative for values of $r$ greater than one mesh-length. The equilibrium structure has not yet been reached at this point. Eighteen inches further downstream, at $x = 57$ in., the scale has decreased considerably, and at large $r$ the correlation has become still more negative. That point is in the equilibrium region, three inches before the end of the distortion. At $x = 75{\cdot}5$, which is 15·5 in.

after the end of the distortion, the scale has increased again but there has not been much change in the correlations at large $r$. Fourteen inches further downstream at $x = 89{\cdot}5$ in., however, the negative values of the correlation have decreased distinctly.

In very disorganized turbulence, e.g. isotropic turbulence, this correlation is expected to be negative and one of the reasons why it changes sign in the distortion may be the suppression of the vortex pair eddies that make it positive in ordinary grid turbulence. This is probably not enough though, because the negative values are quite large and extend over a large range of $r$. The decrease in the negative values after the distortion ends is to be expected if the stress relieving motions initiated in the equilibrium region of the distortion are completing their lives within twenty or thirty inches after the end of the distortion and not many new ones are being formed.

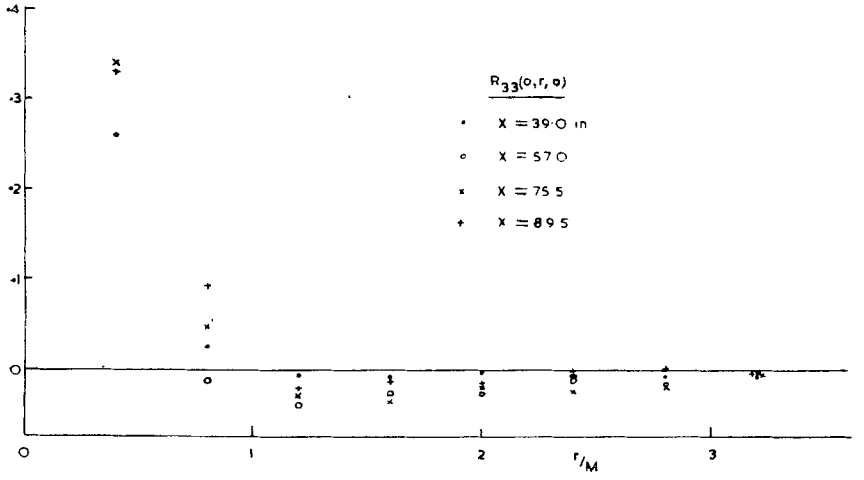


Figure 29. $R_{33}(0, r, 0)$ in and after the distortion.

The observations are thus consistent with the main predictions of the hypothesis of stress relieving motions but it is necessary to assume that when the stress is not too large it is stable, otherwise it is hard to account for the very slow decrease of the anisotropy after the distortion. In the discussion of the wake, it was suggested that the time required for an unstable situation to develop a mixing jet governed the observed average value of the stress. Here we do not have the large intensity gradient of the wake and it may be that when the stress is below a certain value it acts to make the turbulence more homogeneous and is thus stable.

The flatness factors of the distributions of $v$ and $w$ vary considerably over the section of the tunnel but mean values at the end of the distortion are for $v$, 2·97, and for $w$, 3·09. Twenty-six inches after the end of the distortion, the corresponding values are 2·93 and 3·26. The standard deviations were about 0·02. These differ from 3 in the same directions

as the corresponding quantities in the wake. Again, I do not understand why one is larger than 3 and the other smaller, but they show that the turbulence does not consist of patches of stressed and unstressed fluid even after the distortion has ceased, which suggests that if the stress is not too large, it is stable to large stress relieving motions.

It thus seems that the values of the shear coefficient in the wake and in distorted grid turbulence are established by different mechanisms and the fact that the coefficient takes the same value in the two cases is only a coincidence. A constant, but different, value of the shear coefficient is found in several other kinds of turbulent flow. In fully developed two-dimensional channel flow (Laufer 1950) and in the turbulent boundary layer (Klebanoff 1955), the value is nearer 0·3 than 0·4. For an axisymmetric contraction, Uberoi (1956) gives data from which the coefficient $K_1$ can be calculated and it is found to reach an apparent equilibrium value of about 0·8 after a total strain ratio of about 2 in the $(x,y)$-plane.

I am indebted to Dr A. A. Townsend for helpful discussions during the course of this work, and to the Defence Research Board of Canada for financial assistance.

## References

Batchelor, G. K. 1953 *The Theory of Homogeneous Turbulence.* Cambridge University Press.

Batchelor, G. K. & Proudman, I. 1954 *Quart. J. Mech. Appl. Math.* **7**, 83.

Einstein, H. A., & Li, H. 1956 *Proc. Am. Soc. Civil. Eng., Pap.* no. 945 (EM2).

Favre, A. J., Gaviglio, J. J., & Dumas, R. 1957 *J. Fluid Mech.* **2**, 313.

Grant, H. L., & Nisbet, I. C. T. 1957 *J. Fluid Mech.* **2**, 263.

Hamma, F. R., Long, J. D., & Hegarty, J. C. 1957 *J. Appl. Phys.* **28**, 388.

Klebanoff, P. S. 1955 *Nat. Adv. Comm. Aero., Wash., Rep.* no. 1247.

Laufer, J. 1950 *J. Aero. Sci.* **17**, 277.

McPhail, D. C. 1944 *Roy. Aircraft Est., Rep.* no. 1928.

Roshko, A. 1954 *Nat. Adv. Comm. Aero., Wash., Rep.* no. 1191.

Stewart, R. W. 1956 *Can. J. Phys.* **34**, 722.

Stewart, R. W. & Townsend, A. A. 1951 *Phil. Trans.* A, **243**, 359.

Townsend, A. A. 1948 *Aust. J. Sci. Res.* **1**, 161.

Townsend, A. A. 1950 *Phil. Mag.* **41**, 890.

Townsend, A. A. 1954 *Quart. J. Mech. Appl. Math.* **7**, 104.

Townsend, A. A. 1956 *The Structure of Turbulent Shear Flow.* Cambridge University Press.

Uberoi, M. S. 1956 *J. Aero. Sci.* **23**, 754.